Sagi, M. and Fluhr, R. (2001) Superoxide production by plant homologues of the $gp91^{phox}$ NADPH oxidase. modulation of activity by calcium and by tobacco mosaic virus infection. *Plant Physiol.* 126: 1281–1290.

Sanders, D., Brownlee, C. and Harper, J.F. (1999) Communicating with calcium. *Plant Cell* 11: 691–706.

Takezawa, D., Liu, Z.H., An, G. and Poovaiah, B.W. (1995) Calmodulin gene family in potato: developmental and touch-induced expression of the mRNA encoding a novel isoform. *Plant Mol. Biol.* 27: 693–703.

Xu, H. and Heath, M.C. (1998) Role of calcium in signal transduction during the hypersensitive response caused by basidiospore-derived infection of the cowpea rust fungus. *Plant Cell* 10: 585–597.

Yamakawa, H., Katou, S., Seo, S., Mitsuhara, I., Kamada, H. and Ohashi, Y. (2004) Plant MAPK phosphatase interacts with calmodulins. *J. Biol. Chem.* 279: 928–936.

Yamakawa, H., Mitsuhara, I., Ito, N., Seo, S., Kamada, H. and Ohashi, Y. (2001) Transcriptionally and post-transcriptionally regulated response of 13 calmodulin genes to tobacco mosaic virus-induced cell death and wounding in tobacco plant. *Eur. J. Biochem.* 268: 3916–3929.

Yamamoto, Y. (1966) NAD kinase in higher plants. *Plant Physiol.* 41: 523–528.

Zielinski, R.E. (1998) Calmodulin and calmodulin-binding proteins in plants. *Plant Mol. Biol.* 49: 697–725.

(Received February 20, 2004; Accepted July 14, 2004)

The Plant Journal (2004) 40, 131–142 doi: 10.1111/j.1365-313X.2004.02197.x

Crosstalk between elicitor-induced cell death and cell cycle regulation in tobacco BY-2 cells

Yasuhiro Kadota[1], Takashi Watanabe[1], Shinsuke Fujii[1], Katsumi Higashi[2], Toshio Sano[3], Toshiyuki Nagata[4], Seiichiro Hasezawa[3] and Kazuyuki Kuchitsu[1,2,*]

[1]*Department of Applied Biological Science and*

[2]*Genome & Drug Research Center, Tokyo University of Science, 2641 Yamazaki, Noda, Chiba 278-8510, Japan,*

[3]*Department of Integrated Biosciences, Graduate School of Frontier Sciences, University of Tokyo, Kashiwanoha, Kashiwa, Chiba 277-8562, Japan, and*

[4]*Department of Biological Sciences, Graduate School of Science, University of Tokyo, Bunkyo-ku, Tokyo 113-0033, Japan*

Received 5 April 2004; revised 22 June 2004; accepted 13 July 2004.
*For correspondence (fax +81 4 7123 9767; e-mail kuchitsu@rs.noda.tus.ac.jp).

Summary

The molecular links between cell cycle control and the regulation of programmed cell death are largely unknown in plants. Here we studied the relationship between the cell cycle and elicitor-induced cell death using synchronized tobacco BY-2 cells. Flow cytometry and fluorescence microscopy of nuclear DNA, and RNA gel-blot analyses of cell cycle-related genes revealed that the proteinaceous elicitor cryptogein induced cell cycle arrest at the G1 or G2 phase before the induction of cell death. Furthermore, the patterns of cell death induction and defence-related genes were different in different phases of the cell cycle. Constitutive treatment with cryptogein induced cell cycle arrest and cell death at the G1 or G2 phase. With transient treatment for 2 h, cell cycle arrest and cell death were only induced by treatment with the elicitor during the S or G1 phase. By contrast, the elicitor-induced production of reactive oxygen species was observed during all phases of the cell cycle. These results indicate that although recognition of the elicitor signal is cell cycle-independent, the induction of cell cycle arrest and cell death depends on the phase of the cell cycle.

Keywords: cell cycle arrest, elicitor, programmed cell death, tobacco BY-2 cells, synchronous culture.

Introduction

Programmed cell death (PCD) in plants has been identified in a number of developmental processes, including tracheary element formation (Kuriyama and Fukuda, 2002), destruction of cereal aleurone (Fath *et al.*, 2000), endosperm development (Young and Gallie, 2000), embryogenesis (Souter and Lindsey, 2000) and floral organ abortion (Rubinstein, 2000). PCD also has a crucial role in defence responses against microbial attack (Heath, 2000; Jones and Dangl, 1996). The determination of cell fate – that is, whether cells survive, proliferate or undergo PCD – appears to be crucial in developmental processes, cell differentiation and defence responses.

In animal cells, crosstalk between the progression of the cell cycle and apoptosis has been studied extensively. The tumour suppressor protein p53 is stabilized and activated by a variety of cellular stresses such as heat shock, hypoxia, osmotic shock and DNA damage. These, in turn, induce cell cycle arrest in the G1 phase via the transactivation of $p21^{waf}$ protein, which is a potent inhibitor of G1/S CDK (Ko and Prives, 1996; Levine, 1997; Oren, 1994). p53 also activates the expression of an apoptosis-inducing gene, *p53AIP1*, and induces apoptosis (Oda *et al.*, 2000). When the Fas ligand, one of the tumour necrosis factors that induces apoptosis, binds to its receptor Fas, dephosphorylation of retinoblastoma protein (Rb) is induced causing cell cycle arrest in the S phase (N'cho and Brahmi, 2001). Anti-IgM stimulates the multimerization of surface immunoglobulins, which induces cell cycle arrest in the G1 phase and results in apoptosis in a murine B-cell line (Tsubata *et al.*, 1993). This G1 arrest is induced through activation of a CDK inhibitor, $p27^{KIP-1}$ expression, and inactivation of CDK4 and CDK6 expression (Ishida *et al.*, 1995).

Fungal elicitor (oligopeptide elicitor, Pep-25 derived from *Phytophthora sojae*) induces the downregulation of cell

cycle-related genes (Logemann *et al.*, 1995) in parsley cells, implying some link between defence signalling and cell cycle regulation in plants. However, there is no evidence of a direct relationship between the cell cycle and PCD in plants. Furthermore, no genes encoding proteins similar to p53 or related regulators of cell death or the cell cycle have been found in plants (The *Arabidopsis* Genome Initiative, 2000).

We have developed a model system involving elicitor-induced hypersensitive cell death in synchronized tobacco BY-2 cells. Tobacco BY-2 cell suspensions can be synchronized and were therefore used to analyse the mechanisms of cell cycle regulation (Nagata *et al.*, 1992). The proteinaceous elicitor cryptogein, derived from *P. cryptogea*, induces fluxes of Ca^{2+}, NO_3^- and H^+, the production of reactive oxygen species (ROS), protein phosphorylation, cell death and defence-gene activation in various kinds of suspension-cultured tobacco cells (Binet *et al.*, 2001; T. Goh and K. Kuchitsu, Tokyo University of Science, Noda, Japan, unpublished results; Lecourieux-Ouaked *et al.*, 2000; Tavernier *et al.*, 1995; Wendehenne *et al.*, 2002), including BY-2 cells (Kadota *et al.*, 2004a,b; Simon-Plas *et al.*, 2002). Ca^{2+} and anion channel inhibitors both suppress cryptogein-induced cell death, suggesting that induced cell death occurs via a specific signal transduction pathway (Binet *et al.*, 2001; Lecourieux *et al.*, 2002).

In the present study, we examined the relationship between cell cycle and cell death using synchronized tobacco BY-2 cells. Cryptogein induced cell cycle arrest specifically during the G1 or G2 phase prior to the induction of cell death. Furthermore, cell death induction, as well as the accumulation of transcripts of defence-related genes, was strictly dependent on the stage of the cell cycle. Although elicitor recognition occurred during all phases of the cell cycle, downstream events such as elicitor-induced cell death and the inhibition of cell growth occurred only in cells in which the elicitor was recognized during the G1 or S phase. These results show the presence of a relationship between the cell cycle and cell death in plants.

Results

Effect of cryptogein on cell cycle progression

In order to examine the effect of cryptogein on the progression of the cell cycle in BY-2 cells, exponentially growing cells were treated with cryptogein (500 nM). Fluorescence microscopy of 4′,6-diamidino-2-phenylindole (DAPI)-stained cells showed that the elicitor decreased the population of cells in the M phase (Figure 1a). We used flow cytometric analysis to determine the effects of the elicitor on cells in other phases of the cell cycle. The elicitor treatment increased the numbers of cells in the G1 or G2 phase and decreased those in the S phase (Figure 1b), suggesting that the elicitor induced cell cycle arrest during specific phases of the cell cycle. These changes in the cell cycle occurred 6 h after cryptogein application, whereas cell death was detected after 10 h (data not shown). This suggests that cell cycle arrest occurs before cell death.

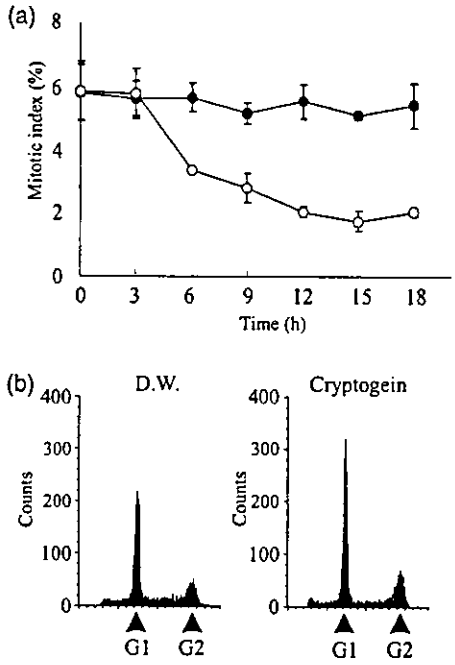

Figure 1. Effect of cryptogein on cell cycle progression in random cultured tobacco BY-2 cells. Cryptogein (500 nM) or distilled water (control) was applied to exponentially growing cells (3 days after sub-culture).
(a) The change of mitotic index after the application of cryptogein (open circles) or distilled water (closed circles). The data represent the average of three independent experiments. Error bars indicate the standard error of the mean ($n = 3$).
(b) Flow cytometric analyses were performed on 3,500 nuclei of the cells 15 h after the application of DW or cryptogein. Representative results of three independent experiments are shown.

Application of cryptogein in the S phase induces cell cycle arrest at the G2 phase

To determine the point in the cell cycle when arrest occurred, cryptogein was applied to BY-2 cells synchronized at the S, late G2 and M phases using the aphidicolin synchronization method (Nagata *et al.*, 1992). Cryptogein was added 0.5 h (S phase), 5.5 h (late G2 phase) and 8.5 h (M phase) after aphidicolin release. Cell cycle progression was monitored using the mitotic index (Figure 2a) and flow cytometry (Figure 2b). Control cells progressed from the S to the G2 phase and subsequently to the M and G1 phases, while cells treated with the elicitor during the S phase showed G2 phase arrest. In contrast, cells treated with cryptogein at the late G2 phase did not show arrest at this stage and progressed to the M/G1 phase. Analysis of mitotic index showed that treatment with cryptogein at the mid-G2 phase (4 h) also did not induce G2 phase arrest (data not shown). After the G1 phase,

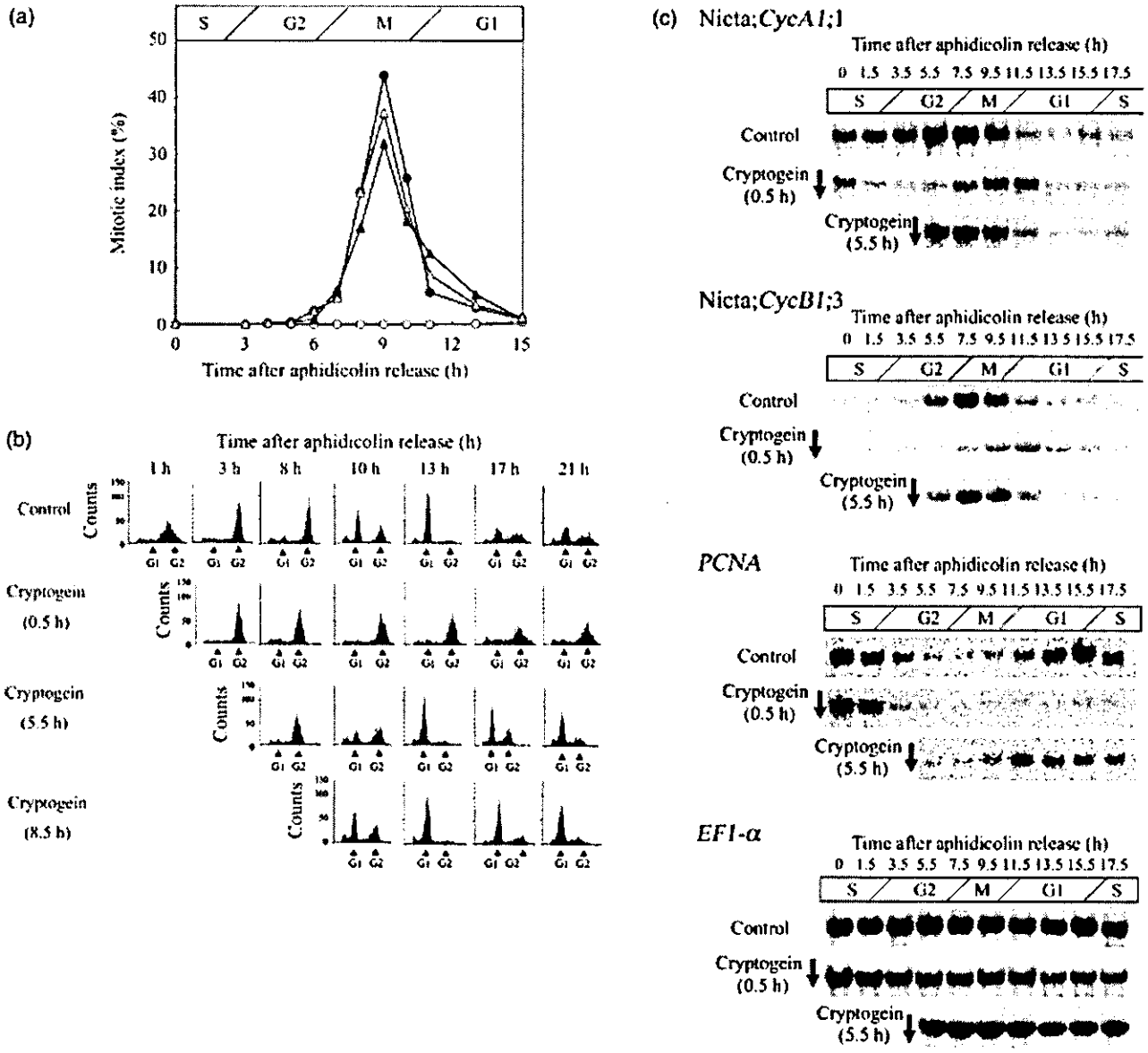

Figure 2. Effect of cryptogein on cell cycle progression of the S, late G2 and M phase cells.
BY-2 cells were synchronized at the S phase by aphidicolin treatment. Representative results of four independent experiments are shown.
(a) The change in the mitotic index of non-treated cells (solid circles) and cells treated with cryptogein at 0.5 h (S phase; open circles), 5.5 h (late G2 phase; solid triangles) or 8.5 h (M phase; open triangles) after release from aphidicolin treatment.
(b) Flow cytometric analyses were performed on 1500 nuclei of non-treated cells (control) and cells treated with cryptogein in S (0.5 h), late G2 (5.5 h) or M (8.5 h) phase.
(c) RNA gel-blot analysis of cell cycle-related gene expression (Nicta;*CycA1*;1, Nicta;*CycB1*;3, and *PCNA*) in non-treated cells (control) and cells treated with cryptogein in S (0.5 h) or late G2 (5.5 h) phase. EF1-α cDNA was used as an internal standard.

a proportion of the cells treated with the elicitor in the late G2 phase seemed to arrest at the G1 phase, because the number of cells that remained in the G1 phase was higher than in untreated cells (17 and 21 h; Figure 2b). By contrast, almost all cells treated with the elicitor during the M phase induced cell cycle arrest at the G1 phase (Figure 2b).

The effect of cryptogein on the accumulation of transcripts of cell cycle-related gene – *A1-type cyclin*, *B1-type cyclin* and proliferating cell nuclear antigen (*PCNA*) – was investigated using RNA gel-blot analysis under the same conditions as in Figure 2(a,b) (Figure 2c). In control cells, the transcripts of Nicta;*CycA1*;1 (*A1-type cyclin*) gene were accumulated from the S phase to the G2/M transition, whereas those of the Nicta;*CycB1*;3 (*B1-type cyclin*) gene were accumulated from the G2 phase until the end of mitosis. By contrast, the accumulation of transcripts of

Nicta;*CycA1;*1 and Nicta;*CycB1;*3 in the cells treated with the elicitor during the S phase was greatly suppressed (Figure 2c). The *PCNA* transcripts were accumulated during the G1-S phase in control cells, while in cells treated with the elicitor during the S phase, *PCNA* transcripts were not detected. These results suggest that the cells treated with the elicitor during the S phase arrested at the G2 phase and did not progress to the G1 phase. Conversely, the cells treated at the late G2 phase induced the accumulation of the transcripts of cyclins in the same manner as the control cells, suggesting that the cell cycle progressed at least as far as the G1 phase (Figure 2c). Cells treated at the late G2 phase induced lower accumulation of *PCNA* transcripts than control cells during the G1 and S phases (13.5–17.5 h). This lower accumulation of *PCNA* transcripts might be due to the fact that some of the cells treated with the elicitor at the late G2 phase arrested during the G1 phase (Figure 2b). This partial cell cycle arrest would then cause fewer cells to progress to the S phase in which the level of *PCNA* transcripts is higher than in the G1 phase.

Application of cryptogein during the M or G1 phase induces cell cycle arrest at the G1 phase

The results described in Figures 1 and 2(b) showed that cryptogein induced cell cycle arrest during both the G1 and G2 phases. For a detailed analysis of the cell cycle-arrest points during the G1 phase, BY-2 cells were highly synchronized during the prometaphase of M phase using the aphidicolin/propyzamide synchronization method (Nagata *et al.*, 1992). Cryptogein was added 0.5 h (M phase) or 5.5 h (G1 phase) after propyzamide release. Cell cycle progression was monitored using the mitotic index (Figure 3a) and flow cytometry (Figure 3b). Control cells progressed from the prometaphase of M phase to the G1 phase, and subsequently to the S phase, the G2 phase and M phase. Cells treated with the elicitor during the M or G1 phase showed G1 arrest (Figure 3a,b). Similarly, cells synchronized by the phosphate starvation method (Sano *et al.*, 1999) showed elicitor-induced G1 arrest (data not shown).

BY-2 cells treated with the elicitor during the M or G1 phase did not induce accumulation of the transcripts of Nicta;*CycA1;*1 or Nicta;*CycB1;*3 (Figure 3c). The accumulation of *PCNA* transcripts was also significantly suppressed in cells treated with the elicitor during the M phase. When we applied the elicitor during the G1 phase, the amount of pre-existing *PCNA* transcripts rapidly decreased.

Elicitor-induced cell death depends on the phase of the cell cycle

To determine the relationship between the cell cycle and the elicitor-induced cell death, we treated BY-2 cells in each phase of the cell cycle with cryptogein. Cryptogein was applied 0.5, 4.5, 6.5, 7.5, 8.5, 9.5 and 13.5 h after aphidicolin release, and cell death was detected using the Evans blue assay. The cells treated with the elicitor during the S phase (0.5 h after aphidicolin release) induced cell death 10 h after aphidicolin release (Figure 4a); 27.3 ± 4.1(SE)% and 65.4 ± 9.5% of cells were stained with Evans blue at 20 and 40 h respectively (Figure 4b).

Although cryptogein was applied to the cells at several time points during the G2 to G1 phase transition (4.5, 6.5, 7.5, 8.5, 9.5 and 13.5 h after aphidicolin release), cell death occurred at a similar time (27.5 h after aphidicolin release; Figure 4a). At 40 h after aphidicolin removal, 26–48% of the cells treated with cryptogein during the G2, M and G1 phases were stained with Evans blue (Figure 4b). These results suggest that the pattern of elicitor-induced cell death changed depending on where the cells were in the cell cycle: cells in the S phase induced cell death rapidly, whereas cells in the G2 or M phase induced cell death at the same time as the cells treated with elicitor in the G1 phase.

Elicitor-induced cell death and the accumulation of transcripts of defence-related genes are strictly regulated in a cell cycle-dependent manner

To study the relationship between cell cycle and defence-related gene activation, the accumulation of several defence-related gene products was measured in cells treated with the elicitor in each phase of the cell cycle. A hypersensitive response-related (*hsr*) gene, *hsr*203J, encoding a serine hydrolase with esterase activity (Baudouin *et al.*, 1997), is postulated to regulate either the establishment or limitation of cell death (Pontier *et al.*, 1998). The expression of the harpin-induced gene *hin1* is correlated with the hypersensitive response (Gopalan *et al.*, 1996). Acidic chitinase (*ACHN*) is a defence gene that breaks down the cell walls of microbes (Linthorst*et al.*, 1990).

Cryptogein was applied 1.5, 5.5, 7.5, 9.5, 11.5 and 13.5 h after aphidicolin release, and the accumulation of the transcripts of these genes was analysed using RNA gel-blot analysis (Figure 5). The transcripts of *hin1*, *hsr203J* and *ACHN* were accumulated in cells treated in the S phase (1.5 h) 4.5 h after aphidicolin release. By contrast, the transcripts of these genes in cells treated with the elicitor at time points from the late G2 to the G1 phase (5.5, 7.5, 9.5, 11.5 and 13.5 h) were accumulated approximately 13.5 h after aphidicolin release. These accumulation patterns of the defence-related gene transcripts were similar to the pattern of cell death induction (Figure 4). These results suggest that both cell death and the accumulation of transcripts of defence-related genes were strictly dependent on the phase of the cell cycle.

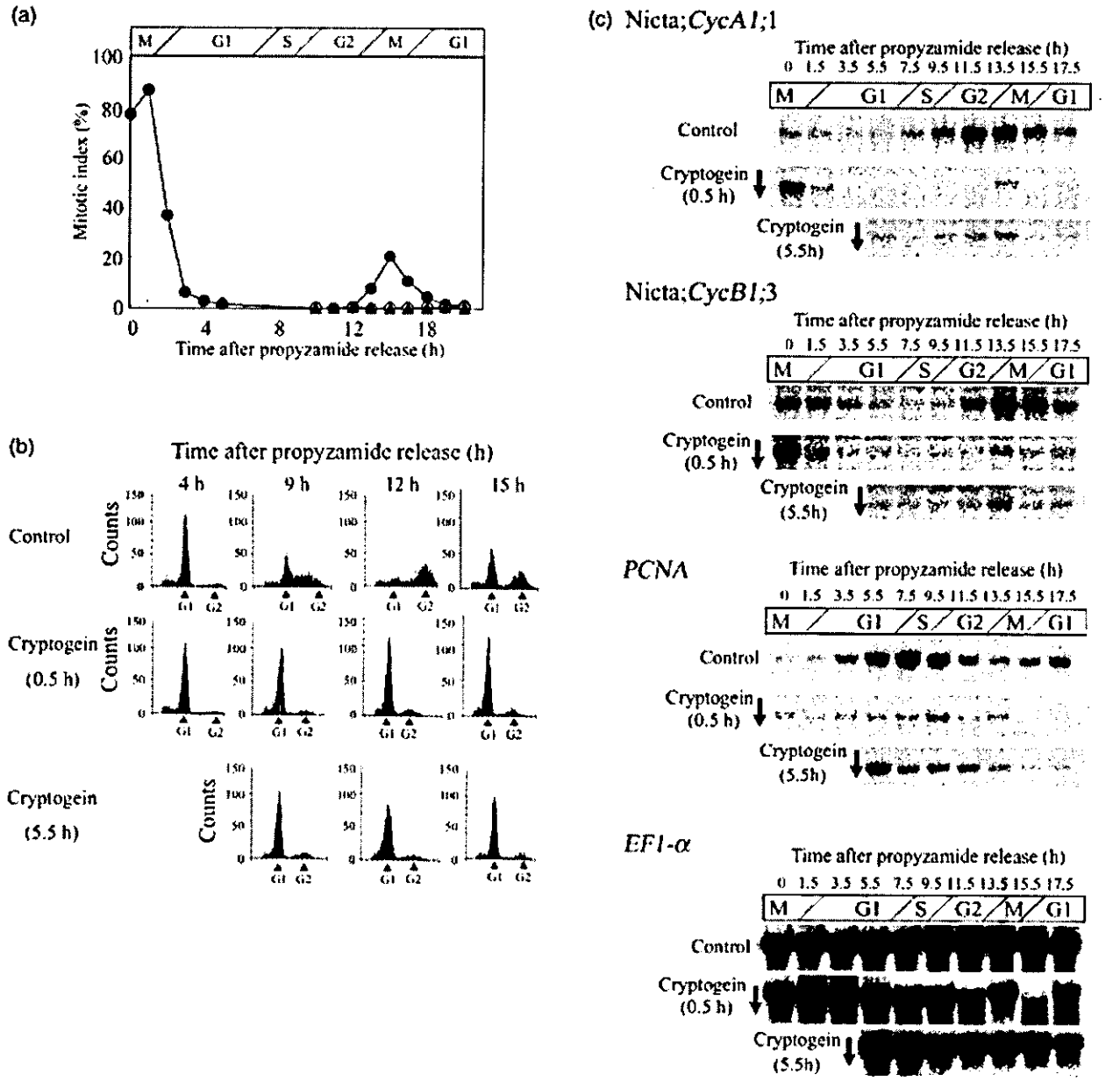

Figure 3. Effect of cryptogein on cell cycle progression of the M and G1 phase cells.
BY-2 cells were synchronized at the M phase using the aphidicolin/propyzamide synchronization method. Representative results of four independent experiments are shown.
(a) The changes in mitotic index of non-treated cells (solid circles) and cells treated with cryptogein (500 nM) at 0.5 h (M phase; open circles) or 5.5 h (G1 phase; solid triangles) after release from propyzamide treatment.
(b) Flow cytometric analysis of non-treated cells (control) and cells treated with cryptogein in the M (0.5 h) or G1 (5.5 h) phase.
(c) RNA gel-blot analysis of cell cycle-related gene expression (Nicta;*CycA1;1*, Nicta;*CycB1;3*, and *PCNA*) in non-treated cells (control) and cells treated with cryptogein in the M (0.5 h) and G1 (5.5 h) phases. EF1-α cDNA was used as an internal standard.

Cell death, growth arrest and cell cycle arrest are induced only at specific phases of the cell cycle

The elicitor-induced cell death and the accumulation of transcripts of defence-related genes were shown to depend strictly on the cell cycle (Figures 4 and 5), suggesting that either recognition or transduction of the elicitor signal is affected by the cell cycle. In order to determine how the cell cycle affects the elicitor-signalling pathway, cells were treated with the elicitor for a limited period of time at each point of the cell cycle. Treatment with the elicitor was required for at least 2 h to induce cell death and growth

(a)

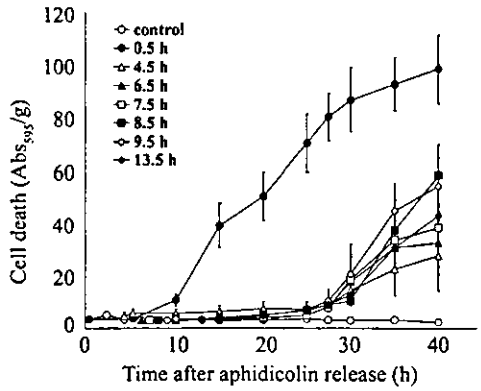

(b)

Time of crytpgein application	Proportion of Evans blue-stained cells (%)		
	0 h	20 h	40 h
Control	0.8 ± 0.3	0.6 ± 0.1	0.7 ± 0.1
0.5 h	–	27.3 ± 4.1	65.4 ± 9.5
4.5 h	–	1.6 ± 0.3	36.7 ± 8.0
6.5 h	–	1.5 ± 0.5	33.6 ± 3.1
7.5 h	–	1.5 ± 0.2	26.8 ± 3.5
8.5 h	–	1.7 ± 0.8	45.6 ± 7.0
9.5 h	–	1.7 ± 0.3	45.4 ± 1.0
13.5 h	–	2.2 ± 0.6	48.1 ± 3.1

Figure 4. Cell cycle-dependent cell death induction. BY-2 cells were synchronized at the S phase by aphidicolin treatment. Cryptogein (500 nM) was applied 0.5, 4.5, 6.5, 7.5, 8.5, 9.5 and 13.5 h after aphidicolin release. The peak of the mitotic index was observed 8–9 h after aphidicolin release in control cells (data not shown), suggesting that cell cycle progression might be similar to that shown in Figure 2.

(a) The time course of cryptogein-induced cell death. Cell death was detected using the Evans blue assay. The data represent the average of three independent experiments. Error bars indicate the standard error of the mean ($n = 3$).

(b) The percentage of cells stained by Evans blue. Approximately 500 cells from each sample were counted using microscopy. The data represent the average of three independent experiments.

arrest in BY-2 cells (Y. Kadota *et al.*, unpublished results). Thus, we treated the cells with cryptogein only for 2 h at each point of the cell cycle in the S and G2 phases (Figure 6a) as well as in the late G2, S and G1 phases (Figure 6b). A 2-h treatment with cryptogein during the S phase induced cell death and growth arrest (Figure 6a). By contrast, cells treated with the elicitor 3 h after aphidicolin release (3–5, 4–6 and 5–7 h) did not show these responses. Flow cytometric analysis showed that almost all of the cells had entered the G2 phase 3 h after aphidicolin release (Figure 2b), suggesting that the drastic difference in the timing of cell death induction and growth arrest is consistent with cell cycle progression from the S phase to the G2 phase.

As cell death induction after elicitor treatment in the late G2, M or G1 phase was weaker than that in the S phase (Figure 4), we applied a higher concentration of cryptogein (1 μM) for the experiment shown in Figure 6(b). Although cryptogein treatment for 2 h in the late G2 or M phase (5–7, 6–8, 7–9 and 9–11 h) did not induce cell death and growth arrest (Figure 6b), cryptogein treatment in the G1 phase (11–13 and 13–15 h) induced these responses.

To confirm whether transient 2-h cryptogein treatment induces G1 or G2 arrest, we analysed the effects of such treatment, during each phase, on cell cycle progression using flow cytometric analysis (Figure 6c). Control cells and cells treated with cryptogein in the late G2 (5–7 h), M (7–9 h) or G1 (11–13 h) phase progressed to the G1 phase 13 h after aphidicolin release, while cells treated with the elicitor in the S phase (0–2 h) showed G2 phase arrest. After the G1 phase, although cells treated in the late G2 (5–7 h) or M (7–9 h) phase showed cell cycle progression similar to the control cells, the cells treated with the elicitor in the G1 phase (11–13 h) induced cell cycle arrest at the G1 phase. Although continuous treatment with cryptogein induced complete cell cycle arrest (Figures 2 and 3), in the case of transient treatment a small portion of the cells treated in the S or G1 phase did not induce cell cycle arrest (Figure 6c). This result might be because 2-h treatment with cryptogein is insufficient to induce cell cycle arrest in all the cells. This is consistent with the result that cell death induced by 2-h transient treatment with the elicitor was also insufficient (Figure 6a).

Continuous treatment with cryptogein from the G2 or M phase induced cell death with similar kinetics to the cells treated with cryptogein from the G1 phase (Figure 4). Conversely, transient 2-h treatment with cryptogein in the G2 or M phase did not induce cell cycle arrest and cell death (Figure 6). Cryptogein treatment from the G2 to just before the G1 phase (5–9 h) also did not induce cell death and cell growth arrest (Y. Kadota *et al.*, unpublished results). These results indicate that cells in the G2 or M phase did not induce cell death and cell cycle arrest; therefore, these cells need to recognize the elicitor after cell cycle progression to the G1 phase to induce these responses.

Elicitor recognition and oxidative burst occur in all phases of the cell cycle

In order to investigate whether elicitor recognition occurs only in the S and G1 phases rather than in all phases of the cell cycle, we analysed the elicitor-induced production of ROS, which is one of the earliest events induced by elicitors (Kuchitsu *et al.*, 1995). Production of the superoxide anion ($^{\cdot}O_2^-$) was monitored using the chemiluminescence of 2-methyl-6-[p-methoxyphenyl]-3,7-dihydroimidazo [1,2-a]pyrazin-3-one (MCLA) (Tampo *et al.*, 1998; Uehara *et al.*, 1993). Cryptogein-induced ROS production occurred during all phases of the cell cycle (Figure 7). ROS production commenced after a 2- to 3-min lag time, and peaked 7–10 min

after elicitor application. These results suggest that the elicitor was recognized during all phases of the cell cycle.

The results shown in Figures 6 and 7 indicate that elicitor recognition occurs during all phases of the cell cycle. During the G2 and M phases, however, cell cycle arrest and cell death are not induced. Consequently, these events are induced only when elicitor recognition occurs in the S or G1 phase.

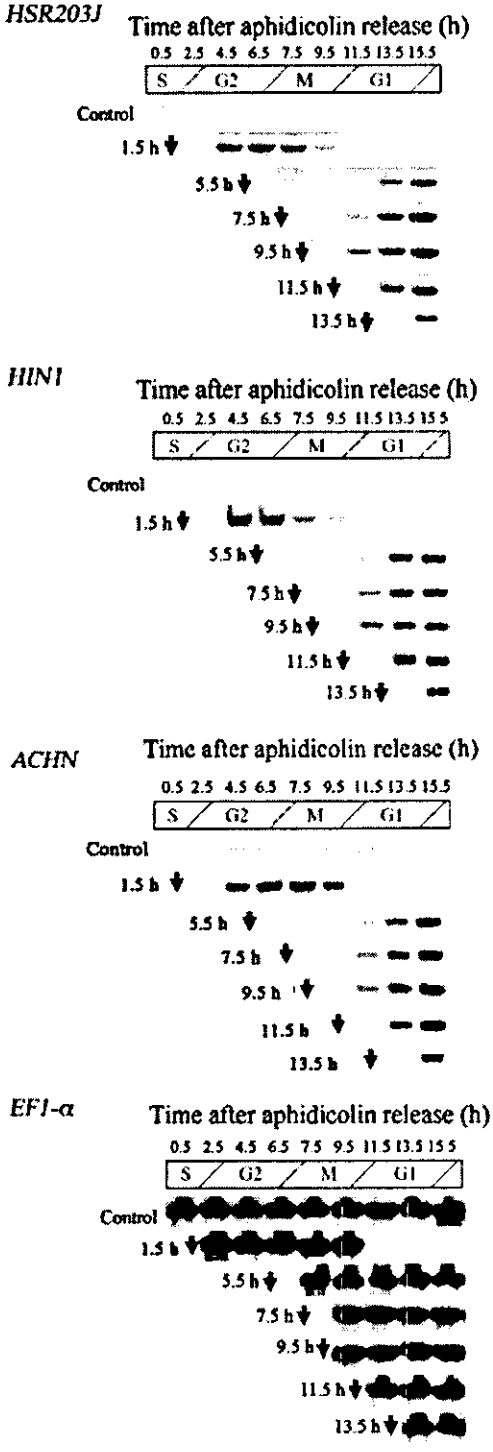

Discussion

The determination of cell fate (proliferation, differentiation or PCD) is crucial during various stages in a plant's life cycle, including development, growth, organogenesis and during stress responses. This study focused on the relationship between the cell cycle and stress-induced cell death in plants. We showed the antithetical relationship between the cell cycle and elicitor-induced defence responses, including death and defence-gene activation. Cell cycle arrest occurred at the G1 or G2 phase before induction of cell death, and the induction of cell death and the accumulation of transcripts of defence-related genes were dependent on where the plant cells were in the cell cycle.

Cryptogein induced cell cycle arrest during the G1 or G2 phase

In several plant species, a relationship has been suggested between stress responses and growth or cell cycle progression. Downregulation of cell cycle-related genes and upregulation of defence genes were induced simultaneously by UV irradiation or elicitor treatment in parsley cells (Logemann *et al.*, 1995), and during menadione-mediated oxidative stress in tobacco cells (Reichheld *et al.*, 1999). A eubacterial flagellin-derived peptidyl elicitor also induced defence-related genes and inhibited growth in *Arabidopsis* seedlings (Gómez-Gómez *et al.*, 1999). *Arabidopsis* mutants expressing defence-related genes constitutively show dwarf phenotype (Bowling *et al.*, 1994). These results may predict the existence of a certain link between cell proliferation and the induction of defence responses. In this study, we showed that a pathogenic elicitor induced cell cycle arrest at the G1 or G2 phase (Figures 2 and 3).

We also studied the expression of cell cycle-related genes. Concomitant with cell cycle arrest, the accumulation of transcripts of the genes involved in the cell cycle such as *A1-type cyclin*, *B1-type cyclin* and *PCNA* was inhibited. These results indicate that the elicitor-induced cell cycle arrest occurred in the G1 or G2 phase. Cyclins are crucial components of the cell cycle machinery as they bind and activate CDKs. *A*1- and *B1-type cyclins* are thought to be

Figure 5. Cell cycle-dependent expression of defence-related genes (*Hsr203J*, *Hin1* and *ACHN*).
BY-2 cells were synchronized at the S phase by aphidicolin treatment. Cryptogein (500 μM) was applied 1.5, 5.5, 7.5, 9.5, 11.5 and 13.5 h after aphidicolin release, and the expression of defence-related genes (*Hin1*, *Hsr203J* and *ACHN*) and *EF1-α* was analysed by RNA gel-blot analysis. EF1-α cDNA was used as an internal standard. The peak of the mitotic index was observed 9 h after aphidicolin release in control cells (data not shown), suggesting that cell cycle progression might be similar to that shown in Figure 2. The figure shows the results of one experiment, which was representative of the three independent experiments.

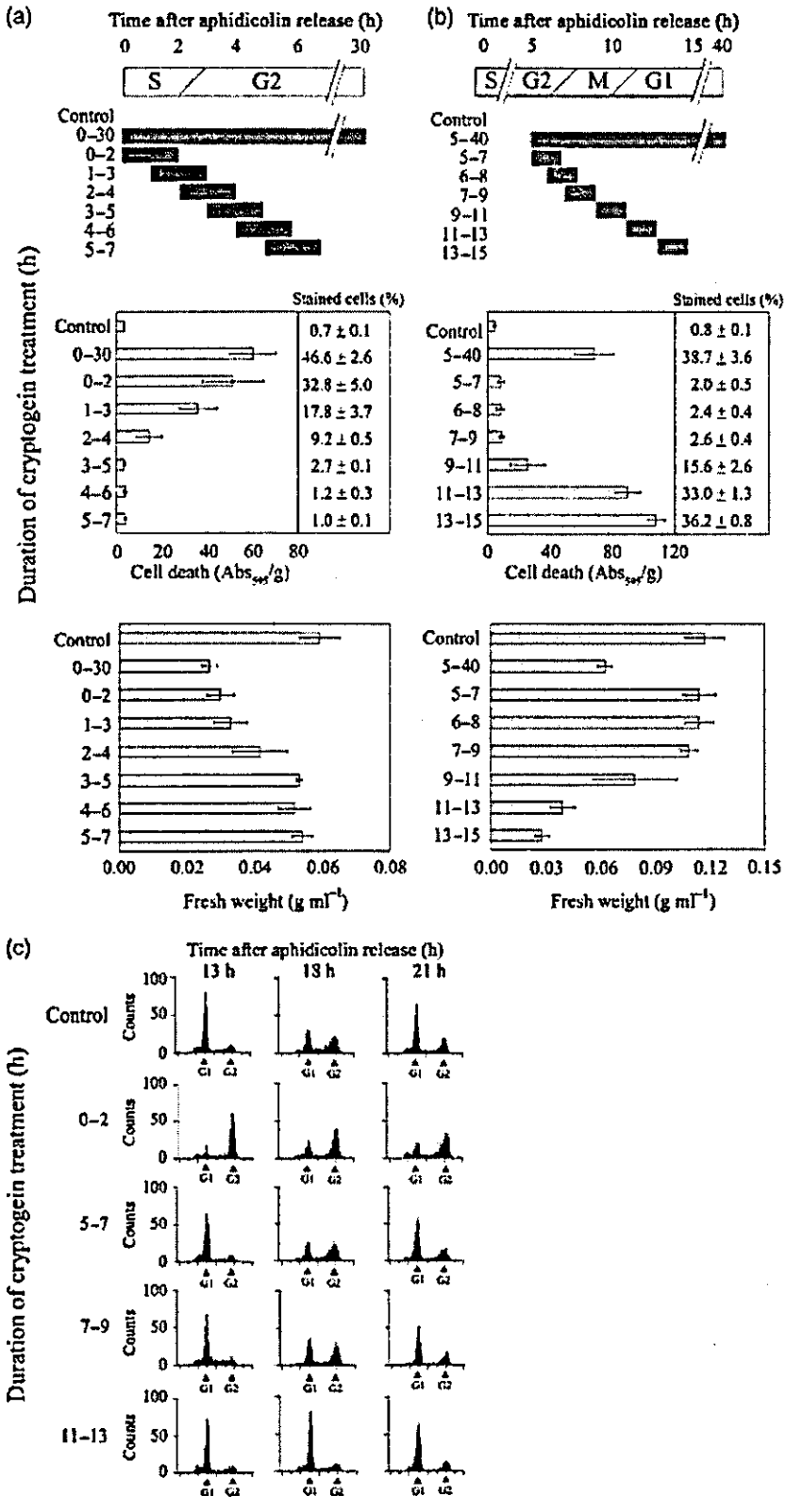

Figure 6. Elicitor-induced cell death and the inhibition of cell growth were only induced when cryptogein recognition occurred in the S or G1 phase. BY-2 cells were synchronized at the S phase by aphidicolin treatment.

(a) Application of cryptogein at the S phase, but not at the G2 phase, induced cell cycle arrest and elicitor-induced cell death. BY-2 cells were treated with cryptogein (500 nM) for 2 h at different phases of the cell cycle from the S to the G2 phase (0–2, 1–3, 2–4, 3–5, 4–6 and 5–7 h after aphidicolin release). Cell death (middle) and fresh weight (lower) were analysed 30 h after aphidicolin release.

(b) Application of the elicitor at the G1 phase, but not at the G2 or M phase, induced cell cycle arrest and cell death. BY-2 cells were treated with cryptogein (1 μM) for 2 h during different phases of the cell cycle from the late G2 to the G1 phase (5–7, 6–8, 7–9, 9–11, 11–13 and 13–15 h after aphidicolin release). Cell death (middle) and fresh weight (lower) were analysed 40 h after aphidicolin release. The peak of the mitotic index was observed 8–9 h after aphidicolin release in control cells (data not shown), suggesting that cell cycle progression might be similar to that shown in Figure 2. The data represent the average of three independent experiments. Error bars indicate the standard error of the mean ($n = 3$).

(c) Flow cytometric analysis of non-treated cells (control) and cells treated with cryptogein for 2 h during the S (0–2 h), late G2 (5–7 h), M (7–9 h) or G1 (11–13 h) phase. Representative results of three independent experiments are shown.

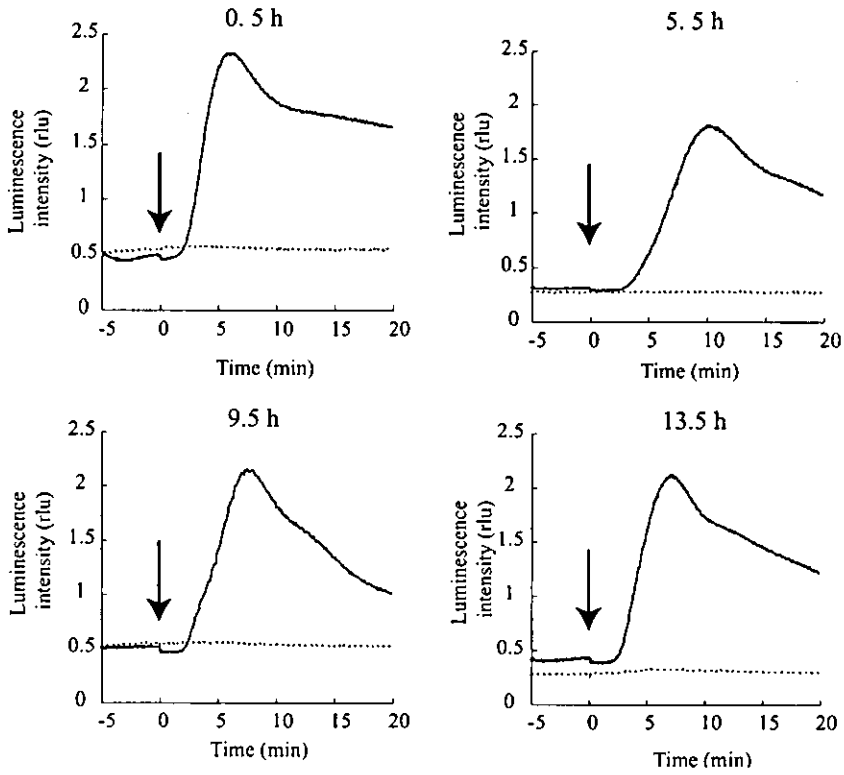

Figure 7. Cryptogein-induced ROS ($^{\cdot}O_2^-$) production occurred during all phases of the cell cycle.
BY-2 cells were synchronized at the S phase by aphidicolin treatment. Cryptogein (500 nM) and distilled water were applied 0.5 h (S phase), 5.5 h (late G2 phase), 9.5 h (M phase) and 13.5 h (G1 phase) after aphidicolin release, and $^{\cdot}O_2^-$ production was followed by MCLA chemiluminescence. Arrows indicate the application of the elicitor or distilled water. The unbroken and broken lines indicate $^{\cdot}O_2^-$ production induced by the elicitor and distilled water respectively. The peak of the mitotic index was observed 9 h after aphidicolin release in control cells (data not shown), suggesting that cell cycle progression might be similar to that shown in Figure 2. The results show one experiment, which is representative of five independent experiments.

involved in the progression from the G2 to the M phase (John *et al.*, 2001; Mironov *et al.*, 1999). Inhibition of cyclin synthesis could account for the distinct cell cycle arrest during the G2 phase. Nevertheless, the roles of these cyclins in plants are still speculative and have been deduced predominantly through studying their respective expression patterns during the cell cycle. An important question for future studies is whether inhibition of their expression is part of the mechanism that triggers elicitor-induced cell cycle arrest, or whether it is a consequence of this arrest.

Cryptogein-induced cell cycle arrest precedes hypersensitive cell death

Only a few previous studies have suggested any relationship between cell death and the cell cycle in plants. Reichheld *et al.* (1999) showed that menadione-mediated oxidative stress slowed DNA replication and delayed the entry of BY-2 cells into mitosis, and that a high menadione concentration induced toxic cell death in plants. In addition, the application of ethylene increased cell mortality at the G2/M phase in tobacco BY-2 cells (Herbert *et al.*, 2001). Evidence for a relationship between the cell cycle and hypersensitive cell death, however, is lacking. In this study, we clearly show for the first time that cryptogein-induced cell cycle arrest at the G1 or G2 phase occurs prior to cell death (Figures 2 and 4). The cells treated with the elicitor during the S phase progressed to the G2 phase 3 h after aphidicolin release and showed complete cell cycle arrest (Figure 2), while cell death induction occurred after 10 h (Figure 4). The cells treated with the elicitor in the G2, M or G1 phase showed cell cycle progression to the G1 phase 13 h after aphidicolin release, followed by complete cell cycle arrest (Figure 2; data not shown), while cell death was observed after 27.5 h. Similar results were also obtained using the aphidicolin/propyzamide synchronization method (data not shown).

After cell cycle arrest, BY-2 cells induce physiological and morphological changes in vacuolar dynamics, disruption of the microtubular network and changes in the permeability of the plasma membrane (T. Goh *et al.*, Tokyo University of Science, Noda, Japan, unpublished results). However, it remains unclear whether cell cycle arrest is necessary for cell death induction. Cell cycle arrest might be necessary, or alternatively cell death and cell cycle arrest might be independent. This issue is crucial in understanding the relationship between the cell cycle and cell death. Experiments using overexpressers of positive cell cycle regulators, such as cyclins, might provide the answer to these questions.

Cryptogein signalling depends on the phase of the cell cycle

Cryptogein induced $^{\cdot}O_2^-$ production in cells during all phases of the cell cycle, confirming that the elicitor was recognized during all stages (Figure 7). By contrast, cell

growth arrest, cell cycle arrest and cell death were induced only when elicitor recognition occurred in the S or G1 phase (Figure 6). These results suggest that the cryptogein-induced signalling pathway depends on the phase of the cell cycle, and the elicitor-signalling pathway might be downregulated in the G2 or M phase. A comparison of various cryptogein-induced signalling events, such as Ca^{2+} signalling and the activation of mitogen-activated protein kinases, in each phase of the cell cycle might provide some answers. Various elicitors have been shown to induce the biphasic production of ROS for several hours (Jabs *et al.*, 1997; Suzuki *et al.*, 1999; Yoshioka *et al.*, 2001). The production of ROS observed at a later stage, following the transient peak reported in this study (Figure 7), might depend on the cell cycle. It is impossible to carry out real-time measurements of $^{\cdot}O_2^-$ production over periods of several hours using the present method, because of depletion of the indicator, MCLA. We are currently improving the method in order to measure the elicitor-induced ROS production at a later stage.

Our results also suggest the possibility that cell division-active sites, such as the meristem, young leaves and seedlings, could not induce strong defence response because they include cells in the G2 or M phase. In fact, young leaves are less sensitive to elicitors than mature leaves (Bailey *et al.*, 1995; Barna and Gyorgyi, 1992). By contrast, almost all of the mesophyll cells of mature leaves are in the G0 or G1 phase (Nagata and Takahash, 1993) and induce strong defence responses and severe cell death as a reaction to elicitors and avirulent pathogens (Ricci *et al.*, 1989). Further experiments will therefore be needed to determine the relationship between the cell cycle and the defence response in intact plants.

The mitotic index of random cultured cells treated with 500 nM cryptogein did not reach zero (Figure 1), suggesting that this concentration of cryptogein does not induce cell cycle arrest in all random cultured cells. Furthermore, the elicitor-induced cell death in random cultured cells was six- to seven-fold lower than that in cells synchronized at the S phase (Y. Kadota *et al.*, unpublished results). These results could be explained by the present finding that the elicitor induced cell death only during a limited segment of the cell cycle (the S and G1 phases). Elicitor treatment of the synchronously cultured cells characterized in this study would provide a novel experimental model system for highly synchronous elicitor-induced cell death, which should be useful in deducing the molecular mechanisms for hypersensitive cell death.

In conclusion, cell cycle arrest occurred before induction of the elicitor-induced cell death, and cell death induction is strictly dependent on the phase of the cell cycle. By further studying this model system, it is possible to gain a better understanding of the molecular relationship between the cell cycle and PCD in plants.

Experimental procedures

Plant material

A tobacco BY-2 (*Nicotiana tabacum* L. cv. Bright Yellow 2) suspension was maintained by weekly dilution (1/100) of cells in modified Linsmaier and Skoog (LS) medium, as described by Nagata *et al.* (1992). The cell suspension was agitated on a rotary shaker at 100 rpm at 28°C in the dark.

Expression and purification of cryptogein

Pichia pastoris (strain GS115) bearing the plasmid pLEP3 was used for cryptogein production. Cryptogein was expressed according to the method described by O'Donohue *et al.* (1996) and was dissolved in distilled water. The concentration of cryptogein was determined using UV spectroscopy with extinction coefficients of 8306 $M^{-1}\,cm^{-1}$ at 277 nm (O'Donohue *et al.*, 1995).

Cell cycle synchronization

A stationary culture of tobacco BY-2 was diluted 1/10 in fresh modified LS medium supplemented with 5 $\mu g\ ml^{-1}$ aphidicolin (Wako Pure Chemical Industries, Ltd., Osaka, Japan). After a 24-h culture, aphidicolin was removed by extensive washes and the cells were re-suspended in fresh medium. When analyses of post-mitotic stages were needed, 0.8 $\mu g\ ml^{-1}$ of propyzamide (Sigma, St Louis, MO, USA) was added before the pre-prophase stage, which was approximately 5 h after removing the aphidicolin. The cultures were then maintained for 4 h before removal of propyzamide through extensive washes.

Determining cell division of BY-2 cells

Cell division percentages were determined by measuring the mitotic index after staining the cells with DAPI and observing them under a fluorescence microscope.

Flow cytometric analysis

Flow cytometric analysis was performed according to the manufacturer's protocol. One millilitre of cell suspension was centrifuged at 1000 × *g* for 1 min. About 100 µl of Solution A (PARTEC High Resolution Kit type P; Partec GmbH, Münster, Germany) was added to the pellet of the cell suspension. The cells were chopped with a razor blade and then incubated for 10 min at room temperature. The nuclei were separated from the cells by filtering the mixture through a 100-µm nylon filter. For staining, 400 µl of Solution B was added to the nuclear solution. Fluorescence intensity was measured by flow cytometry (Ploidy analyser PA; Partec GmbH). Counts that had a low fluorescence intensity included fluorescence from artificially fragmented DNA produced during the extraction of the nuclei. We therefore disregarded counts below a cut-off value of a much lower fluorescence intensity than that of the nuclei at the G1 phase.

RNA extraction and Northern blot analysis

Total RNA was extracted from each frozen sample of cells using the Trizol Reagent according to the manufacturer's protocol (Invitrogen Co., Carlsbad, CA, USA). Denatured total RNA (15 µg) was electrophoresed on a 2% agarose gel containing 5.5%

formaldehyde and transferred to a Hybond-N membrane (Amersham-Pharmacia Biotech, Little Chalfont, UK). Hybridization was performed at 65°C in phosphate buffer (500 mM Na-phosphate, pH 7.2, 1 mM EDTA, 1% BSA, 7% SDS) to random primed [^{32}P] probes for Nicta;*CycA1;1*, Nicta;*CycB1;3*, *PCNA* (Ito *et al.*, 1997; Sekine *et al.*, 1999; Setiady *et al.*, 1995) and *EF*1-α (Kumagai *et al.*, 1995) cDNA from tobacco. The hybridization signal was visualized with a Bioimage analyser (BAS-2000; Fuji Film, Tokyo, Japan) and Typhoon 9210 (Amersham-Pharmacia Biotech).

Cell death assay

One millilitre of the cell suspension was incubated with 0.05% Evans blue (Sigma) for 15 min and then washed to remove the unabsorbed dye. The selective staining of dead cells with Evans blue depends upon extrusion of the dye from living cells via the intact plasma membrane. The dye passes through the damaged membrane of dead cells and accumulates as a blue protoplasmic stain (Turner and Novacky, 1974). Dye that had been absorbed by dead cells was extracted in 50% methanol with 1% SDS for 1 h at 60°C and quantified by absorbance at 595 nm. We also measured the fresh weight by using 10 ml of the same culture, and the value measured by Evans blue was divided by the fresh weight to average the cell volume.

Measurement of O_2^- production

A BY-2 cell suspension was washed and re-suspended in fresh growth medium 30 min before measurement. The cells were then treated with 2 μM MCLA (Molecular Probes, Eugene, OR, USA), and the O_2^--dependent luminescence was measured with a Lumicounter 2500 (Microtech Nition, Chiba, Japan).

Acknowledgements

The authors thank Drs Kaoru Suzuki, Masami Sekine, Masaki Ito and Fumi Kumagai for the generous gifts of cDNA clones of ACHN, Hsr203J and Hin1, a cDNA clone of Nicta;*CycA1;1*, cDNA clones of Nicta;*CycB1;3* and PCNA, and a cDNA clone of EF1-α, respectively. We are also grateful to Drs Kaoru Suzuki, Masaaki Umeda, Masaki Ito, Masami Sekine, Seisuke Kimura, Toyoki Amano, Mr Arata Yoneda, Mr Natsumaro Kutsuna and Mr Yoshihisa Oda for valuable suggestions and critical reading of the manuscript. We thank Ms Ryoko Saitou for technical assistance. We also thank Professor Jean-Claude Pernollet for providing us with cryptogein. This work was supported in part by a Grant-in-Aid for the Research for the Future Program and Scientific Research (B) (No. 14340251) from the Japan Society for the Promotion of Science to K. K. and Grants-in-Aid for Scientific Research in Priority Areas from the Ministry of Education, Science, Culture, Sports, and Technology, Japan to K. K. (No. 13039015).

References

Bailey, B.A., Avni, A. and Anderson, D. (1995) The influence of ethylene and tissue age on the sensitivity of xanthi tobacco leaves to a *Trichoderma viride* xylanase. *Plant Cell Physiol.* **36**, 1669–1676.

Barna, B. and Gyorgyi, B. (1992) Resistance of young versus old tobacco leaves to necrotrophs, fusaric acid, cell wall-degrading enzymes and autolysis of membrane lipids. *Physiol. Mol. Plant Physiol.* **40**, 247–257.

Baudouin, E., Charpenteau, M., Roby, D., Marco, Y., Ranjeva, R. and Ranty, B. (1997) Functional expression of a tobacco gene related to the serine hydrolase family-esterase activity towards short-chain dinitrophenyl acylesters. *Eur. J. Biochem.* **248**, 700–706.

Binet, M., Humbert, C., Lecourieux, D., Vantard, M. and Pugin, A. (2001) Disruption of microtubular cytoskeleton induced by cryptogein, an elicitor of hypersensitive response in tobacco cells. *Plant Physiol.* **125**, 564–572.

Bowling, S.A., Guo, A., Cao, H., Gordon, A.S., Klessig, D.F. and Dong, X. (1994) A mutation in *Arabidopsis* that leads to constitutive expression of systemic acquired resistance. *Plant Cell*, **6**, 1845–1857.

Fath, A., Bethke, P., Lonsdale, J., Meza-Romero, R. and Jones, R. (2000) Programmed cell death in cereal aleurone. *Plant Mol. Biol.* **44**, 255–266.

Gómez-Gómez, L., Felix, G. and Boller, T. (1999) A single locus determines sensitivity to bacterial flagellin in *Arabidopsis thaliana*. *Plant J.* **18**, 277–284.

Gopalan, S., Wei, W. and He, S.Y. (1996) *hrp* gene-dependent induction of *hin1*: a plant gene activated rapidly by both harpins and the avrPto gene-mediated signal. *Plant J.* **10**, 591–600.

Heath, M.C. (2000) Hypersensitive response-related death. *Plant Mol. Biol.* **44**, 321–334.

Herbert, R.J., Vilhar, B., Evett, C., Orchard, C.B., Rogers, H.J., Davies, M.S. and Francis, D. (2001) Ethylene induces cell death at particular phases of the cell cycle in the tobacco TBY-2 cell line. *J. Exp. Bot.* **52**, 1615–1623.

Ishida, T., Kobayashi, N., Tojo, T., Ishida, S., Yamamoto, T. and Inoue, J. (1995) CD40 signaling-mediated induction of Bcl-XL, Cdk4, and Cdk6. Implication of their cooperation in selective B cell growth. *J. Immunol.* **155**, 5527–5535.

Ito, M., Marie-Claire, C., Sakabe, M., Ohno, T., Hata, S., Kouchi, H., Hashimoto, J., Fukuda, H., Komamine, A. and Watanabe, A. (1997) Cell-cycle-regulated transcription of A- and B-type plant cyclin genes in synchronous cultures. *Plant J.* **11**, 983–992.

Jabs, T., Tschope, M., Colling, C., Hahlbrock, K. and Scheel, D. (1997) Elicitor-stimulated ion fluxes and O_2^- from the oxidative burst are essential components in triggering defence gene activation and phytoalexin synthesis in parsley. *Proc. Natl Acad. Sci. USA*, **94**, 4800–4805.

John, P.C., Mews, M. and Moore, R. (2001) Cyclin/Cdk complexes: their involvement in cell cycle progression and mitotic division. *Protoplasma*, **216**, 119–142.

Jones, A.M. and Dangl, J.L. (1996) Logjam at the Styx: programmed cell death in plants. *Trends Plant Sci.* **1**, 114–119.

Kadota, Y., Goh, T., Tomatsu, H., Tamauchi, R., Higashi, K., Muto, S. and Kuchitsu, K. (2004a) Cryptogein-induced initial events in tobacco BY-2 cells: pharmacological characterization of molecular relationship among cytosolic Ca^{2+} transients, anion efflux and production of reactive oxygen species. *Plant Cell Physiol.* **45**, 160–170.

Kadota, Y., Furuichi, T., Ogasawara, Y., Goh, T., Higashi, K., Muto, S. and Kuchitsu, K. (2004b) Identification of putative voltage-dependent Ca^{2+} -permeable channels involved in cryptogein-induced Ca^{2+} transients and defence responses in tobacco BY-2 cells. *Biochem. Biophys. Res. Commun.* **317**, 823–830.

Ko, L.J. and Prives, C. (1996) p53: puzzle and paradigm. *Genes Dev.* **10**, 1054–1072.

Kuchitsu, K., Kosaka, H., Shiga, T. and Shibuya, N. (1995) EPR evidence for generation of hydroxyl radical triggered by *N*-acetylchitooligosaccharide elicitor and a protein phosphatase inhibitor in suspension-cultured rice cells. *Protoplasma*, **188**, 138–142.

Kumagai, F., Hasezawa, S., Takahashi, Y. and Nagata, T. (1995) The involvement of protein synthesis elongation factor 1 in the organization of microtubules on the perinuclear region during the cell cycle transition from M phase to G1 phase in tobacco BY-2 cells. *Bot. Acta.* **108**, 467–473.

Kuriyama, H. and Fukuda, H. (2002) Developmental programmed cell death in plants. *Curr. Opin. Plant Biol.* **5**, 568–573.

Lecourieux, D., Mazars, C., Pauly, N., Ranjeva, R. and Pugin, A. (2002) Analysis and effects of cytosolic free calcium increases in response to elicitors in *Nicotiana plumbaginifolia* cells. *Plant Cell*, **14**, 2627–2641.

Lecourieux-Ouaked, F., Pugin, A. and Lebrun-Garcia, A. (2000) Phosphoproteins involved in the signal transduction of cryptogein, an elicitor of defence reactions in tobacco. *Mol. Plant Microbe Interact.* **13**, 821–829.

Levine, A.J. (1997) p53, the cellular gatekeeper for growth and division. *Cell*, **88**, 323–331.

Linthorst, H.J., van Loon, L.C., Van Rossum, C.M., Mayer, A., Bol, J.F., Van Roekel, J.S., Meulenhoff, E.J. and Cornelissen, B.J. (1990) Analysis of acidic and basic chitinases from tobacco and petunia and their constitutive expression in transgenic tobacco. *Mol. Plant Microbe Interact.* **3**, 252–258.

Logemann, E., Wu, S.C., Schroder, J., Schmelzer, E., Somssich, I.E. and Hahlbrock, K. (1995) Gene activation by UV light, fungal elicitor or fungal infection in *Petroselinum crispum* is correlated with repression of cell-cycle-related genes. *Plant J.* **8**, 865–876.

Mironov, V., Veylder, L.D., Montagu, M.V. and Inzé, D. (1999) Cyclin-dependent kinases and cell division in plants – the nexus. *Plant Cell*, **11**, 509–522.

N'cho, M. and Brahmi, Z. (2001) Evidence that Fas-induced apoptosis leads to S phase arrest. *Hum Immunol.* **62**, 310–319.

Nagata, T. and Takahashi, Y. (1993) Auxin-induced activation of DNA synthesis via par genes in tobacco mesophyll protoplasts. In *Molecular and Cell Biology of the Plant Cell Cycle* (Ormond, J.C. and Francis, D., eds). Dordrecht: Kluwer Academic, pp. 133–141.

Nagata, T., Nemoto, Y. and Hasezawa, S. (1992) Tobacco BY-2 cell line as the 'HeLa' cell in the cell biology of higher plants. *Inter. Rev. Cytol.* **132**, 1–30.

Oda, K., Arakawa, H., Tanaka, T. *et al.* (2000) p53AIP1, a potential mediator of p53-dependent apoptosis, and its regulation by Ser-46-phosphorylated p53. *Cell*, **102**, 849–862.

O'Donohue, M.J., Gousseau, H., Huet, J.C., Tepfer, D. and Pernollet, J.C. (1995) Chemical synthesis, expression and mutagenesis of a gene encoding beta-cryptogein, an elicitin produced by *Phytophthora cryptogea*. *Plant Mol. Biol.* **27**, 577–586.

O'Donohue, M.J., Boissy, G., Huet, J.C., Nespoulous, C., Brunie, S. and Pernollet, J.C. (1996) Overexpression in *Pichia pastoris* and crystallization of an elicitor protein secreted by the phytopathogenic fungus, *Phytophthora cryptogea*. *Protein Expr. Purif.* **8**, 254–261.

Oren, M. (1994) Relationship of p53 to the control of apoptotic cell death. *Semin. Cancer Biol.* **5**, 221–227.

Pontier, D., Tronchet, M., Rogowsky, P., Lam, E. and Roby, D. (1998) Activation of *hsr203*, a plant gene expressed during incompatible plant-pathogen interactions, is correlated with programmed cell death. *Mol. Plant Microbe Interact.* **11**, 544–554.

Reichheld, J.P., Vernoux, T., Lardon, F., Montagu, M.V. and Inzé, D. (1999) Specific checkpoints regulate plant cell cycle progression in response to oxidative stress. *Plant J.* **17**, 647–656.

Ricci, P., Bonnet, P., Huet, J.C., Sallantin, M., Beauvais-Cante, F., Bruneteau, M., Billard, V., Michel, G. and Pernollet, J.C. (1989) Structure and activity of proteins from pathogenic fungi *Phytophthora* eliciting necrosis and acquired resistance in tobacco. *Eur. J. Biochem.* **183**, 555–563.

Rubinstein, B. (2000) Regulation of cell death in flower petals. *Plant Mol. Biol.* **44**, 303–318.

Sano, T., Kuraya, Y., Amino, S. and Nagata, T. (1999) Phosphate as a limiting factor for the cell division of tobacco BY-2 cells. *Plant Cell Physiol.* **40**, 1–8.

Sekine, M., Ito, M., Uemukai, K., Maeda, Y., Nakagami, H. and Shinmyo, A. (1999) Isolation and characterization of the E2F-like gene in plants. *FEBS Lett.* **460**, 117–122.

Setiady, Y.Y., Sekine, M., Hariguchi, N., Yamamoto, T., Kouchi, H. and Shinmyo, A. (1995) Tobacco mitotic cyclins: cloning, characterization, gene expression and functional assay. *Plant J.* **8**, 949–957.

Simon-Plas, F., Elmayan, T. and Blein, J.P. (2002) The plasma membrane oxidase NtrbohD is responsible for AOS production in elicited tobacco cells. *Plant J.* **31**, 137–147.

Souter, M. and Lindsey, K. (2000) Polarity and signalling in plant embryogenesis. *J. Exp. Bot.* **51**, 971–983.

Suzuki, K., Yano, A. and Shinshi, H. (1999) Slow and prolonged activation of the p47 protein kinase during hypersensitive cell death in a culture of tobacco cells. *Plant Physiol.* **119**, 1465–1472.

Tampo, Y., Tsukamoto, M. and Yonaha, M. (1998) The antioxidant action of 2-methyl-6-(p-methoxyphenyl)-3,7-dihydroimidazo[1,2-alpha]pyrazin-3-one (MCLA), a chemiluminescence probe to detect superoxide anions. *FEBS Lett.* **430**, 348–352.

Tavernier, E., Wendehenne, D., Blein, J.P. and Pugin, A. (1995) Involvement of free calcium in action of cryptogein, a proteinaceous elicitor of hypersensitive reaction in tobacco cells. *Plant Physiol.* **109**, 1025–1031.

The *Arabidopsis* Genome Initiative (2000) Analysis of the genome sequence of the flowering plant *Arabidopsis thaliana*. *Nature*, **408**, 796–815.

Tsubata, T., Wu, J. and Honjo, T. (1993) B-cell apoptosis induced by antigen receptor crosslinking is blocked by a T-cell signal through CD40. *Nature*, **364**, 645–648.

Turner, J.G. and Novacky, A. (1974) The quantitative relation between plant and bacterial cells involved in the hypersensitive reaction. *Phytopathology*, **64**, 885–890.

Uehara, K., Maruyama, N., Huang, C.K. and Nakano, M. (1993) The first application of a chemiluminescence probe, 2-methyl-6-[p-methoxyphenyl]-3,7-dihydroimidazo[1,2-a]pyrazin-3-one (MCLA), for detecting O_2^- production, *in vitro*, from Kupffer cells stimulated by phorbol myristate acetate. *FEBS Lett.* **335**, 167–170.

Wendehenne, D., Lamotte, O., Frachisse, J.M., Barbier-Brygoo, H. and Pugin, A. (2002) Nitrate efflux is an essential component of the cryptogein signaling pathway leading to defence responses and hypersensitive cell death in tobacco. *Plant Cell*, **14**, 1937–1951.

Yoshioka, H., Sugie, K., Park, H.J., Maeda, H., Tsuda, N., Kawakita, K. and Doke, N. (2001) Induction of plant gp91 phox homolog by fungal cell wall, arachidonic acid, and salicylic acid in potato. *Mol. Plant Microbe Interact.* **14**, 725–736.

Young, T.E. and Gallie, D.R. (2000) Programmed cell death during endosperm development. *Plant Mol. Biol.* **44**, 283–301.

Plant Cell Physiol. 45(6): 693–702 (2004)

Identification of a Putative Voltage-Gated Ca^{2+}-permeable Channel (OsTPC1) Involved in Ca^{2+} Influx and Regulation of Growth and Development in Rice

Takamitsu Kurusu [1], Yasuhiro Sakurai [1], Akio Miyao [3], Hirohiko Hirochika [3] and Kazuyuki Kuchitsu [1, 2, 4]

[1] *Department of Applied Biological Science, Tokyo University of Science, 2641 Yamazaki, Noda, Chiba, 278-8510 Japan*
[2] *Genome & Drug Research Center, Tokyo University of Science, 2641 Yamazaki, Noda, Chiba, 278-8510 Japan*
[3] *Department of Molecular Genetics, National Institute of Agrobiological Sciences, Kannondai, Tsukuba, Ibaraki, 305-8602 Japan*

Cytosolic free Ca^{2+} serves as an important second messenger participating in signal transduction of various environmental stresses. However, molecular bases for the plasma membrane Ca^{2+} influx and its regulation remain largely unknown. We here identified a gene (*OsTPC1*) encoding a putative voltage-gated Ca^{2+} channel from rice, ubiquitously expressed in mature leaves, shoots and roots as well as in cultured cells. OsTPC1 rescued the Ca^{2+} uptake activity and growth rate of a yeast mutant *cch1*. To elucidate its physiological roles, we generated transgenic rice plants and cultured cells overexpressing *OsTPC1* mRNA. Furthermore, a retrotransposon (*Tos17*) insertional knockout mutant of *OsTPC1* was isolated. *OsTPC1*-overexpressing cells showed hypersensitivity to excess Ca^{2+} but higher growth rate under Ca^{2+} limitation, while growth of the *OsTPC1*-knockout cultured cells was less sensitive to extracellular free Ca^{2+} concentration, suggesting that OsTPC1 has Ca^{2+} transport activity across the plasma membrane. *OsTPC1*-overexpressing plants showed reduced growth and abnormal greening of roots. Growth of *Ostpc1* seedlings was comparable to the control on agar plates, while significantly reduced in adult plants. These results suggest that OsTPC1 functions as a Ca^{2+}-permeable channel involved in the regulation of growth and development.

Keywords: Calcium ion — Ion channel — Plasma membrane — Retrotransposon — Rice — Transport.

Abbreviations: $[Ca^{2+}]_{ext}$, extracellular free calcium ion concentration; $[Ca^{2+}]_{cyt}$, cytosolic free calcium ion concentration; RACE, rapid amplification of cDNA ends; RT-PCR, reverse transcriptase-PCR; TPC1, two-pore channel 1.

Introduction

Mobilization of cytosolic free Ca^{2+} is essential for transduction and conversion of signals, such as, light, touch, cold shock, pathogen attack, plant hormones into adapted biological responses (Sanders et al. 2002, White and Broadley 2003, and references therein) as well as for growth and development including root growth and elongation of pollen tubes (Li et al. 1999, Foreman et al. 2003). Elevation of cytosolic free calcium ion concentration ($[Ca^{2+}]_{cyt}$) is postulated to be mediated by Ca^{2+} channels located on the plasma membrane and endomembranes. In animal cells, many voltage-dependent Ca^{2+}-permeable channels have been identified which function in the transduction of sensory input and signal transduction (Benitah et al. 2002). In plants, membrane depolarization is involved in various signal transduction pathways (Ward et al. 1995, White 2000). Electrophysiological studies revealed the existence of plasma membrane Ca^{2+}-permeable channels activated by membrane depolarization or hyperpolarization in response to environmental stimuli (reviewed in White 2000). They are postulated to play pivotal roles at early steps of a variety of signal transduction networks, such as abscisic acid-induced stomatal closure (Hamilton et al. 2000, Pei et al. 2000), defense responses (Klüsener et al. 2002), tip-growth in rhizoid cells (Taylor et al. 1996) and growth of root apex (Kiegle et al. 2000).

Very little is known, however, about their molecular basis. In animals, typical α-subunits of voltage-gated Ca^{2+} channels are composed of four homologous domains, while no genes encoding these Ca^{2+} channels are found in plants. Ishibashi et al. (2000) recently reported a novel type of a putative voltage-gated Ca^{2+} channel (two-pore channel 1; TPC1) in rat and described existence of a homologous sequence in the *Arabidopsis* genome. Furuichi et al. (2001) cloned the gene (*AtTPC1*) and suggested its possible involvement in $[Ca^{2+}]_{cyt}$ elevation caused by sucrose-induced membrane depolarization. The existence of homologs in other various plant species was also suggested (White et al. 2002). However, physiological roles of the TPC1 family channels still remain mostly unknown in plants and even in animals.

Rice is a useful model plant for agriculturally important crops and monocots, whose entire genomic sequencing has been completed (Shimamoto and Kyozuka 2002). A retrotransposon (*Tos17*) insertional mutagenesis-mediated gene knockout system has recently been established as a powerful tool (Hirochika 1999, Hirochika 2001).

In the present study, we have identified a TPC1 homolog in the rice genome and developed its overexpressors as well as *Tos17* insertional knockout mutant (*Ostpc1*). Ca^{2+} transport activity and effects on growth and development were characterized both in planta and in suspension-cultured cells to elucidate its physiological roles.

[4] Corresponding author: E-mail, kuchitsu@rs.noda.tus.ac.jp; Fax, +81-4-7123-9767.

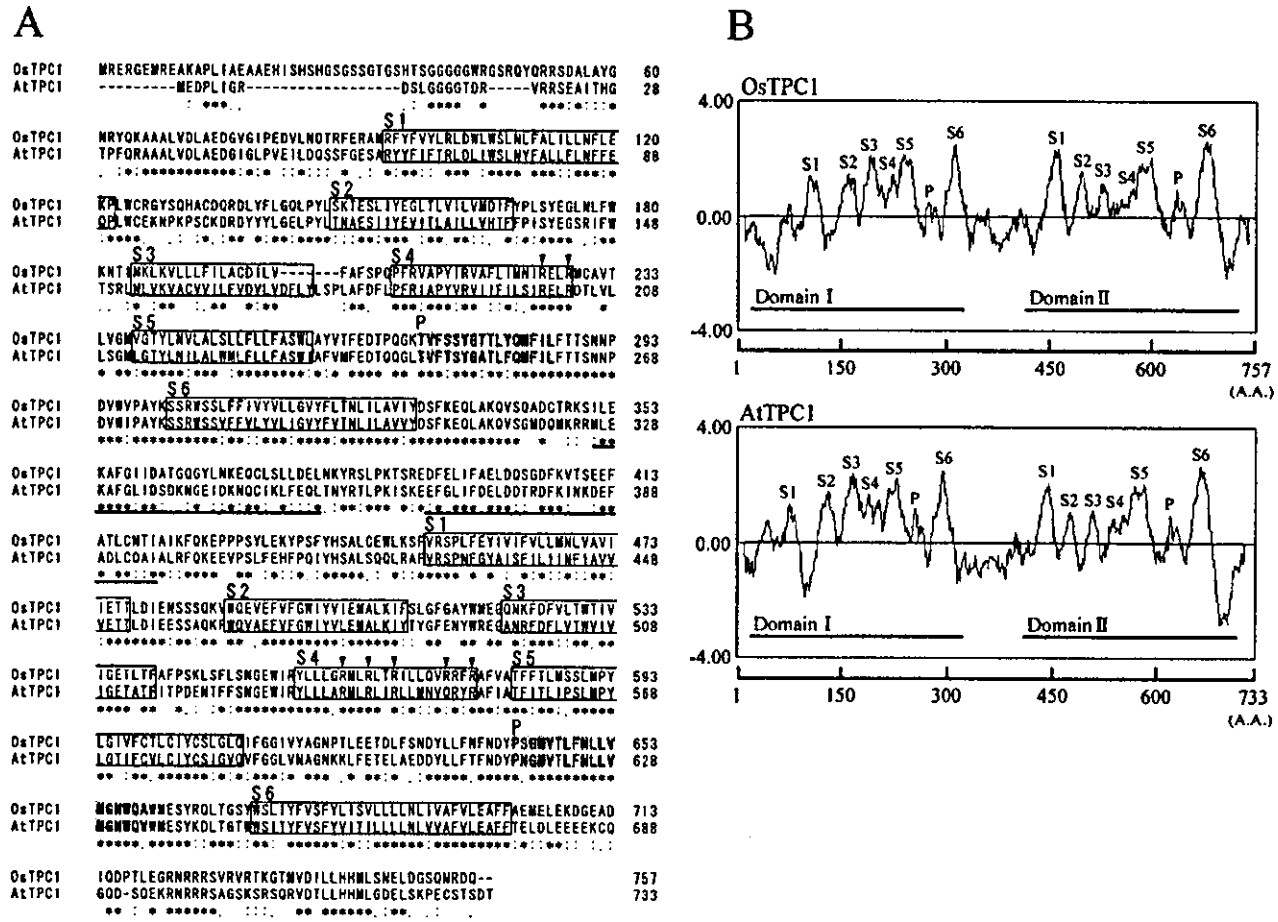

Fig. 1 The rice OsTPC1. (A) Alignment of the predicted amino acid sequences of rice *OsTPC1* and *Arabidopsis AtTPC1*. Asterisks indicate identical or conserved residues in the whole sequence in the alignment. Colons indicate conserved substitutions. Dots indicate semi-conserved substitutions. Twelve putative transmembrane segments are boxed. Two putative pore loops are gray boxed. Arginine residues (R) located at each third position of S4 segments are indicated with arrowheads. Two putative EF-hand motifs are underlined. (B) Kyte and Doolittle hydropathy plot. The six hydrophobic segments (S1–S6) and a pore loop segments (P) in each domain are indicated.

Results

We searched for homologs of Ca^{2+} channels and transporters in the rice genome, and found a novel gene homologous to the rat and *Arabidopsis TPC1* (Ishibashi et al. 2000, Furuichi et al. 2001), which was designated as *OsTPC1* (GenBank Accession No. AB071014). The full-length cDNA was obtained by using RACE-PCR method, which encoded a polypeptide of 757 amino acids with calculated molecular mass of 87,019.

The predicted protein showed 60.4% homology in amino acid sequence compared to AtTPC1, and two transmembrane segments (S1-S6) and two pore loops (p) between S5 and S6 are especially more conserved in comparison with other regions (Fig. 1A). The predicted secondary structure was also similar to AtTPC1 (Fig. 1B). The two EF-hand motifs were found by PFSCAN prediction (http://hits.isb-sib.ch/cgi-bin/PFSCAN) in the linker domain that connects domain I to domain II (Fig. 1A). Southern blot analysis of genomic DNA as well as database search of the whole genome (Rice BLAST; http://riceblast.dna.affrc.go.jp/) indicated that no homologous gene for OsTPC1 was present in rice (data not shown). Expression of the *OsTPC1* mRNA was detected at a similar level ubiquitously in calli, mature leaves and shoots except for roots where its expression was weaker (Fig. 2).

Complementation of a yeast Ca^{2+}-requiring mutant

To confirm that OsTPC1 has Ca^{2+} uptake activity, we carried out yeast complementation analysis by using *Saccharomyces cerevisiae CCH1* defective mutant. CCH1 is a plasma membrane protein, which has significant sequence homology with the α-subunit of animal L-type Ca^{2+} channels. Growth of *cch1* mutant is suppressed in a low Ca^{2+} medium (Fischer et al. 1997). Expression of *OsTPC1* in a *cch1* mutant strain, K927, partially restored its growth under Ca^{2+} limitation (Fig. 3A). The $^{45}Ca^{2+}$ uptake activity of the transformant was higher than that of its parent strain W303-1A (Fig. 3B). These results indicate that OsTPC1 rescued Ca^{2+} transport activity across the plasma membrane of *cch1* mutant.

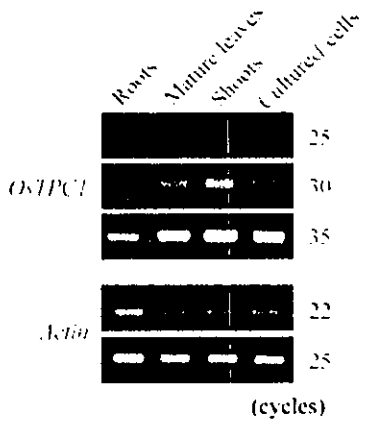

Fig. 2 Expression of *OsTPC1* in rice tissues. First-strand cDNA was synthesized from the total RNA extracted from various tissues and amplified indicated cycles by RT-PCR as described in Materials and Methods. *Actin* cDNA was used as a control DNA. PCR products were analyzed by agarose gel electrophoresis.

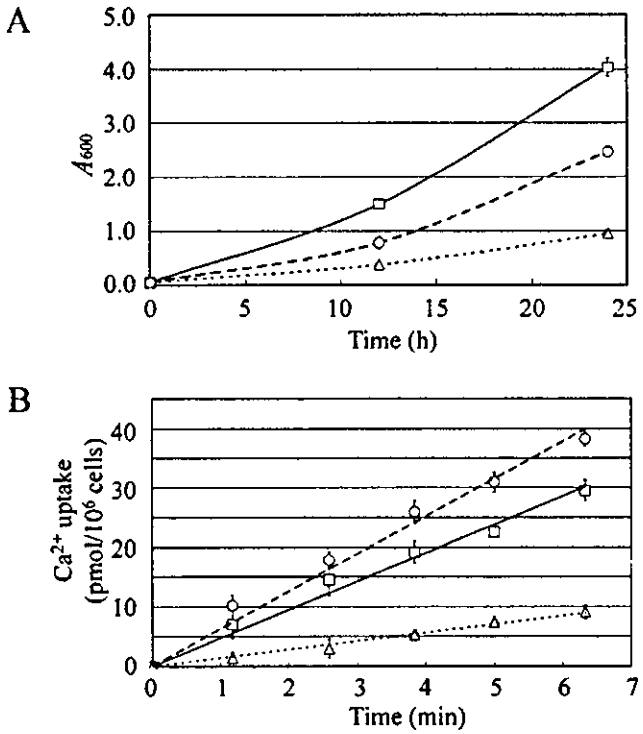

Fig. 3 OsTPC1 rescues both growth rate and Ca^{2+} uptake activity of yeast *cch1* mutant. (A) Exponentially growing cells of strains W303-1A (wild type)/pYES2, K927 (*cch1*)/pYES2 and (*cch1*)/pYES2-*OsTPC1* were transferred into SGal-Ca^{2+} medium, and the cell growth (A_{600}) was measured at the indicated times. Square, W301-1A (wild type)/pYES2; circle, K927 (*cch1*)/pYES2-*OsTPC1*; triangle, K927 (*cch1*)/pYES2. Vertical bars represent SE ($n = 3$). (B) Ca^{2+} uptake was measured by the method described by Eilam and Chernichovsky (1987) with slight modifications. Square, W301–1A (wild type)/pYES2; circle, K927 (*cch1*)/pYES2-*OsTPC1*; triangle, K927 (*cch1*)/pYES2. Vertical bars represent SE ($n = 3$).

Overexpression of OsTPC1

To reveal physiological roles of OsTPC1, the deduced open reading frame was introduced into calli in the sense orientation under the control of cauliflower mosaic virus 35S promoter (Fig. 4A) by means of *Agrobacterium*-mediated transformation (Tanaka et al. 2001). Six independent lines of transgenic plants (T_1 generation) were generated. As a control, three independent lines in which the β-glucuronidase (GUS) gene was introduced were simultaneously investigated. Expression of *OsTPC1* mRNA in T_1 transgenic lines was analyzed by RT-PCR. As shown in Fig. 4B, *OsTPC1* mRNA highly accumulated in all *35S::OsTPC1* transgenic lines. Three independent overexpressing lines (S2-3, S2-4 and S2-5) were used for further experiments.

Isolation of the Tos17 insertional mutant of OsTPC1

To further dissect the in vivo function of the *OsTPC1* gene, we screened 39,744 mutant lines induced by insertion of *Tos17* by PCR and identified one *Tos17* insertional mutant (*Ostpc1*) line (NF1041). In this line, *Tos17* was found to be inserted in the forward orientation near the end of the 11th exon (Fig. 5A), and an alternative mRNA derived from the splicing of exon 10 to exon 12, skipping exon 11, was expressed (Fig. 5B, C). Function of the product of the alternative mRNA was examined by the yeast complementation. *OsTPC1* cDNA isolated from the mutant line did not complement the yeast *cch1* mutant (Fig. 5D). R2 populations were used for further experiments.

Effect of OsTPC1 expression level on Ca^{2+} sensitivity in suspension-cultured cells

As a first step of functional analyses of OsTPC1, we tested whether its expression level affect Ca^{2+} sensitivity of growth in suspension-cultured cells. As shown in Fig. 6, the growth rate of *OsTPC1* overexpressors was lower than that of the control line in the regular medium (Ca^{2+}: 3 mM) and was remarkably reduced under high Ca^{2+} concentration (30 mM). On the other hand, the *OsTPC1* overexpressors showed higher growth rate under Ca^{2+} limitation (0–0.5 mM) than the control line.

In contrast to the *OsTPC1* overexpressors, growth inhibition under high Ca^{2+} concentration (60 mM) was rescued by *Ostpc1* mutation. Ca^{2+} sensitivity of *Ostpc1* for growth was markedly lower than the control (Fig. 7B).

Effects of OsTPC1 expression level on growth and development in planta

We examined whether plant growth and development is affected by the expression level of *OsTPC1*. As shown in Fig. 4C and D, the *OsTPC1* overexpressors showed remarkably slowed growth and reduced fertility in adult plants. Limited growth rate was observed throughout all developmental stages.

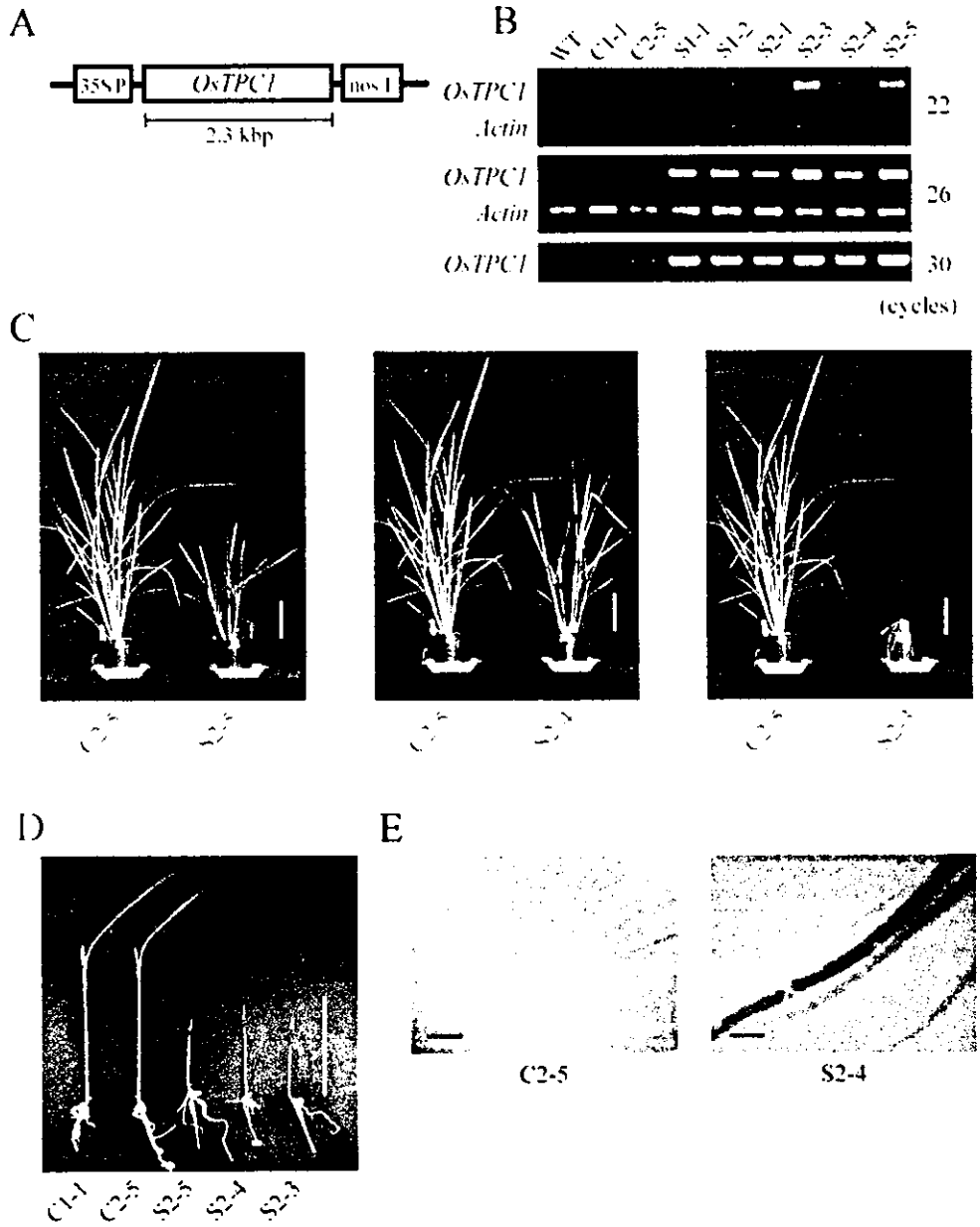

Fig. 4 Phenotypes of plants overexpressing *OsTPC1* cDNA. (A) The *OsTPC1* expression vector for rice transformation. 35S P, CaMV 35S promoter; *OsTPC1*, ORF regions (2,274 bp in size) for *OsTPC1* cDNA; nos T, terminator sequence of the gene for nopaline synthase. *35S::GUS* was used as vector controls. (B) RT-PCR analysis of *OsTPC1* in the plants with sense *OsTPC1*. *Actin* cDNA was used as a control. (C) Phenotype of overexpressing *OsTPC1* lines (T_1) at adult stage. Plants were grown for 60 d in the greenhouse. Right: plant overexpressing *OsTPC1* mRNA and left: control plant overexpressing *GUS* gene. White bars indicate 10 cm. (D) Phenotype of overexpressing *OsTPC1* lines (T_1) at seedling stage. Seedlings were grown for 10 d in the MS medium (16 h light/8 h darkness, 28°C). White bars indicate 10 cm. (E) Root greening observed in overexpressing *OsTPC1* lines (T_1). Seedlings were grown for 14 d in the MS medium (continuous light, 28°C). Red bars indicate 1 mm. Control lines: C1-1 and C2-5, *OsTPC1* overexpressors: S2-3, S2-4 and S2-5.

These phenotypes were exhibited in all six independent T_1 transgenic lines and the expression level of the *OsTPC1* transcripts in the *35S::OsTPC1* plants well correlated with the severity of the phenotypes (Fig. 4B, C). *OsTPC1* overexpressing lines showing severe phenotype also displayed a dwarf phenotype with dark green leaves in adult plants, and green-colored roots in the seedling stage under light conditions (Fig. 4E). The chlorophyll content in these roots was ±4.72 μg (g FW)$^{-1}$, while it was ±0.101 μg (g FW)$^{-1}$ in control roots, indicating that overexpression of *OsTPC1* resulted in abnormal greening of roots. Root greening was not observed in the plants grown under dark conditions (data not shown). One line (S2-3),

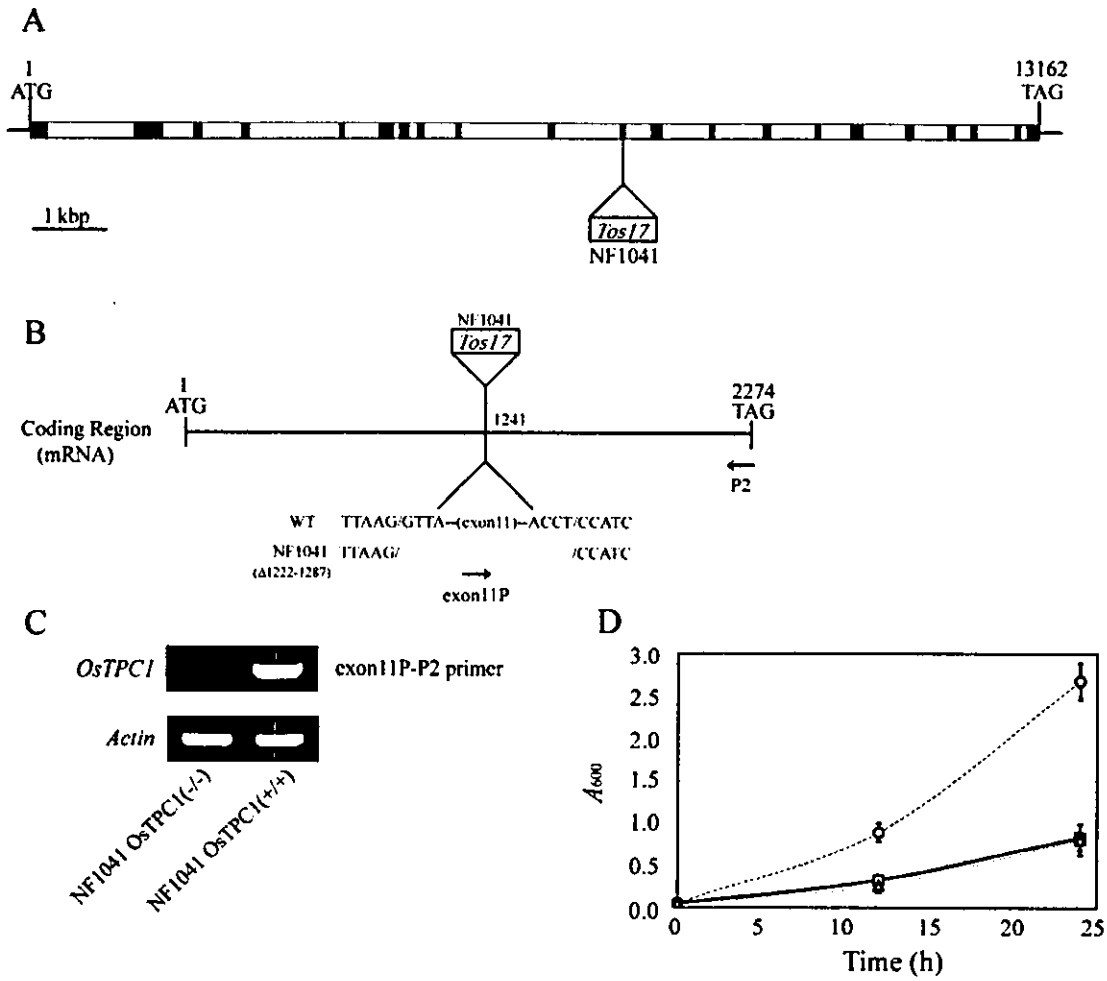

Fig. 5 Isolation of *Tos17* insertional mutant of the *OsTPC1*. (A) The structure of the *OsTPC1* gene and insertion site of *Tos17* in the *OsTPC1* gene of the mutant line (NF1041). The exon and intron regions of *OsTPC1* are presented as closed and open bars, respectively. (B) A schematic representation of *OsTPC1* mRNA and the location of the deletion in the *Ostpc1* mutant. The approximate locations of primer sequences are shown by arrows. (C) PCR analysis of *OsTPC1* mRNA in *Ostpc1* and wild type. PCR products generated by using primers exon11P and P2, which amplify the mRNA region derived from the splicing of exon 11 to exon 21. (D) Yeast complementation analysis using *Ostpc1* cDNA. Square, K927 (*cch1*)/pYES2; circle, K927 (*cch1*)/pYES2-*OsTPC1*; triangle, K927 (*cch1*)/pYES2-*Ostpc1*. Vertical bars represent SE ($n = 3$).

which showed the most severe phenotype, died immediately after transplantation to soil (Fig. 4C).

Adult plants of *Ostpc1* showed slightly reduced growth rate under normal growth conditions (Fig. 7A). Germination and growth of *Ostpc1* seedlings was comparable to the control in the MS medium both in the presence or absence of sucrose. However, its growth became reduced after transplantation to soil to grow in a greenhouse (data not shown), suggesting that the knockout line shows stress hypersensitivity.

To examine whether this phenotype shown in Fig. 7A was due to the insertion of *Tos17* in *OsTPC1*, we examined cosegregation of the *Tos17*-induced *Ostpc1* mutation with the mutant phenotype. Sixty-four R2 plants derived from three R1 heterozygous plants were examined and perfect cosegregation was observed. These results strongly suggest that the observed mutant phenotype was caused by the insertion of *Tos17* in *OsTPC1*.

Discussion

In spite of physiological importance of voltage-gated Ca^{2+} channels in a broad range of signaling pathways in plants, very little is known about their molecular identity. We here identified OsTPC1 as a putative voltage-gated Ca^{2+} channel in rice. Characterization of transgenic plants and suspension-cultured cells of its overexpressors as well as knockouts indicated its Ca^{2+} transport activity in suspension-cultured cells and possible functions in growth and development as well as stress responses in planta.

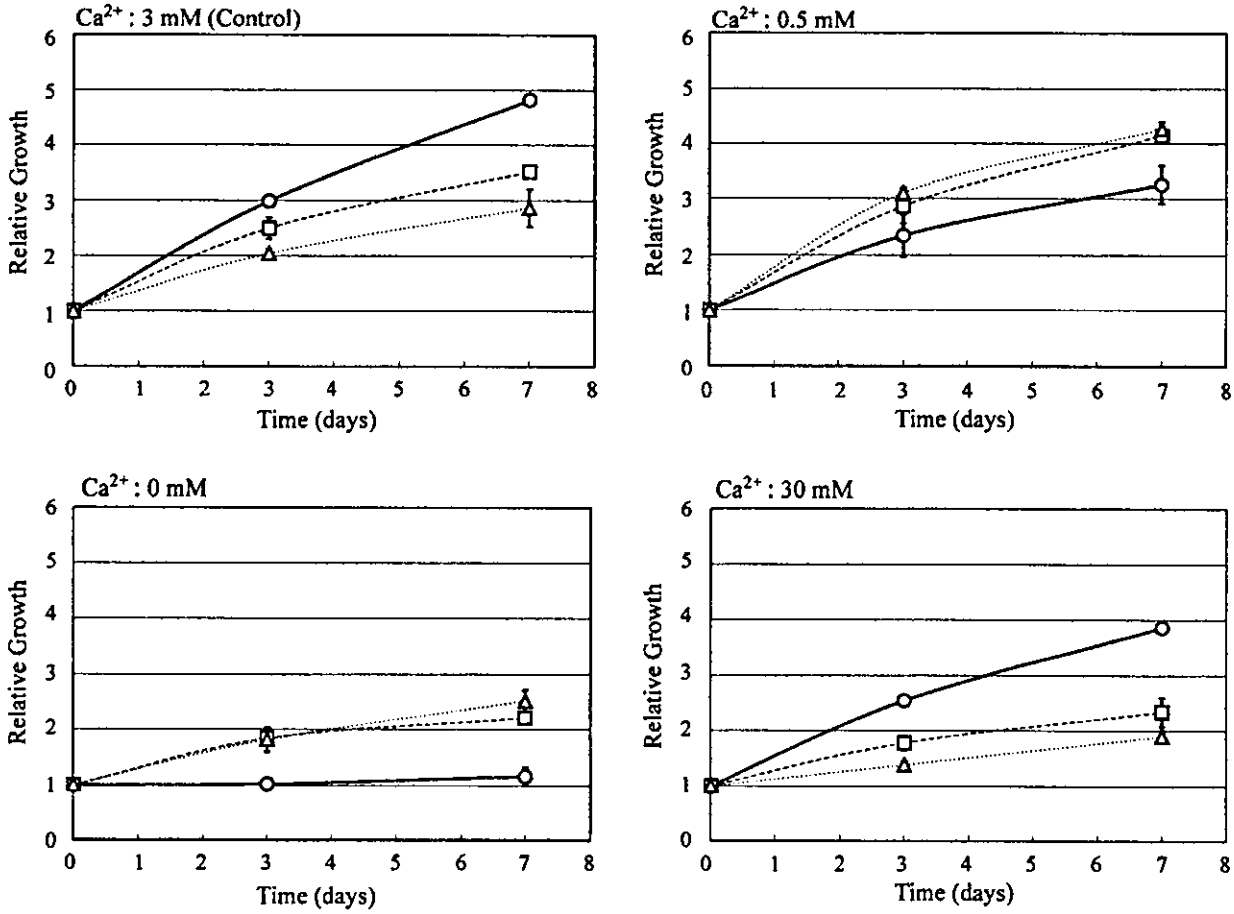

Fig. 6 Ca^{2+} sensitivity of *OsTPC1*-overexpressing transgenic rice cells. Seven-day-old cultured cells were assayed in this experiment. Cells (0.5 g FW) were transferred to standard medium without or supplemented with $CaCl_2$ and incubated. After culturing for 3 or 7 d, fresh weight was measured. Circle, C2-5; square, S2-4; triangle, S2-5. Vertical bars represent SE ($n = 3$).

OsTPC1 encodes a putative voltage-gated channel capable of transporting Ca^{2+} across the plasma membrane in yeast cells

The hydropathy profile of OsTPC1 shows a significant structural similarity with AtTPC1 and TPC1 from rat as well as the halves of the general structure of α-subunits of L-type voltage-gated Ca^{2+} permeable channels. The predicted protein has strong similarity to AtTPC1 (60.4%) and showed the highest homology with rat TPC1 (25.2%) among Ca^{2+} permeable channels in animals. Two EF-hand motifs were found in the linker domain (Fig. 1A) as seen in some mammalian L-type Ca^{2+} channels, in which binding of Ca^{2+} to the motifs lead to the inhibition in the channel activities (Peterson et al. 2000). Ca^{2+} channel activity of OsTPC1 may be downregulated by $[Ca^{2+}]_{cyt}$ as a negative feedback mechanism.

The yeast Ca^{2+}-requiring *cch1* mutation was rescued by expressing *OsTPC1* (Fig. 3A, B) as shown with *AtTPC1* (Furuichi et al. 2001), suggesting that OsTPC1 have Ca^{2+} transport activity across the plasma membrane. Since both of the two S4 segments of OsTPC1 contained positively charged arginine residues located at each third position (Fig. 1A) and this structure is conserved among mammalian voltage-gated Ca^{2+} channels to function as a voltage sensor (Fozzard and Hanck 1996), OsTPC1 may well be voltage-gated. Though detection of functional current of the rat TPC1 have been unsuccessful in heterologously expressed CHO cells and *Xenopus* oocyte (Ishibashi et al. 2000), it should be an important future research subject to electrophysiologically test the Ca^{2+} channel activity of OsTPC1 as well as its voltage dependency.

Expression level of OsTPC1 determines Ca^{2+} sensitivity in suspension-cultured cells

Effects of *OsTPC1* expression levels on Ca^{2+} sensitivity of growth in suspension-cultured cells were analyzed. *OsTPC1* overexpressors showed higher growth rate under low Ca^{2+} concentration (Fig. 6), whereas growth of the *Ostpc1* was less sensitive to $[Ca^{2+}]_{ext}$ (Fig. 7B). These results suggest that OsTPC1 translocates substantial amount of Ca^{2+} across the plasma membrane, and is one of the major factors affecting Ca^{2+} sensitivity at least in suspension-cultured cells.

Previous electrophysiological studies indicate existence of several types of plasma membrane Ca^{2+}-permeable channels activated by membrane depolarization or hyperpolarization

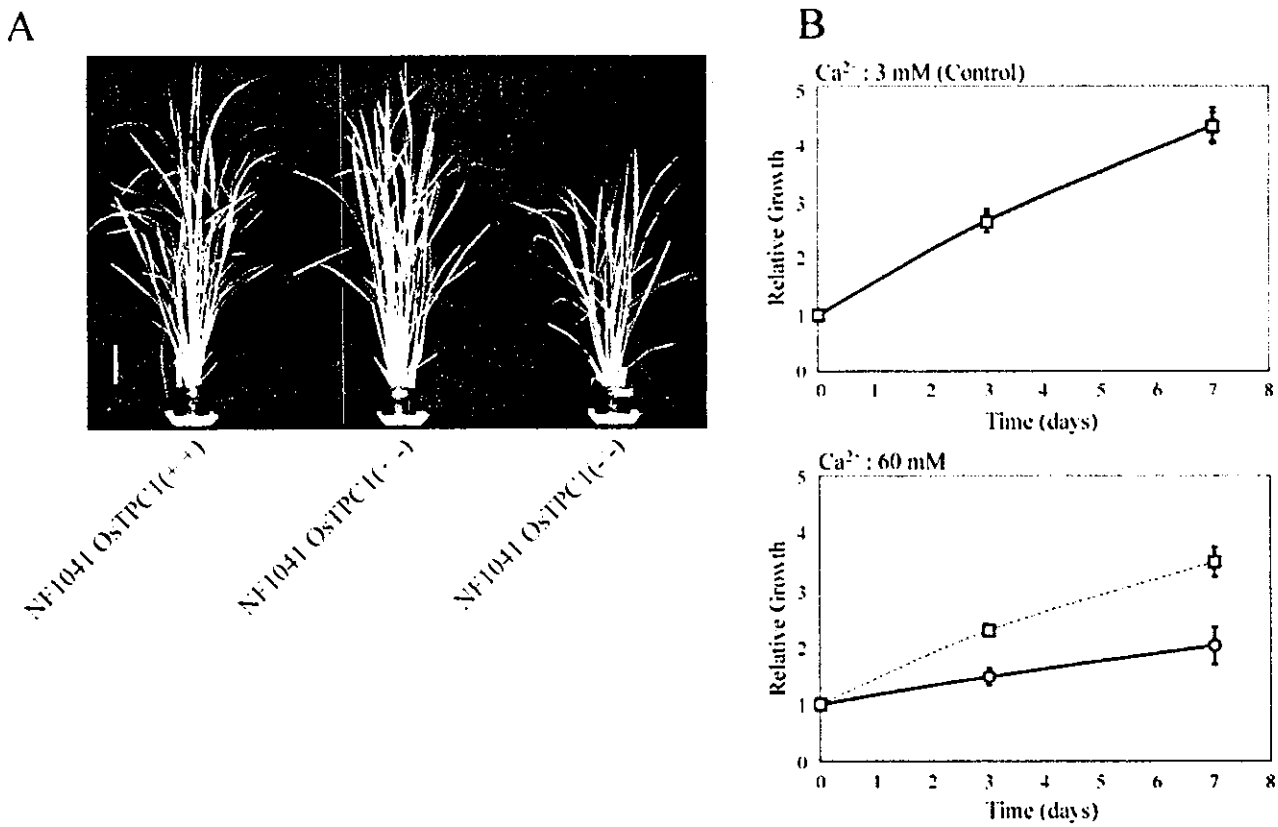

Fig. 7 Phenotypes and Ca^{2+} sensitivity of *Ostpc1* mutant. (A) Phenotype of *Ostpc1* mutant at adult stage. Plants were grown for 90 d in the greenhouse. NF 1041 WT (left), NF1041 heterozygote (middle) and NF1041 homozygote (right). Bars indicate 10 cm. (B) *Ostpc1* suspension-cultured cells render Ca^{2+} sensitivity. Seven-day-old-cultured cells were assayed. Cells (0.5 g FW) were transferred to the standard medium or that supplemented with $CaCl_2$ (60 mM) and grown. After culturing for 3 or 7 d, fresh weight was measured. Circle, NF1041 WT; square, NF1041 homozygote. Vertical bars represent SE ($n = 3$).

(reviewed in White 2000). However, no other genes except for the TPC1 family have been found as a candidate for voltage-gated Ca^{2+} permeable channels in plants (Very and Sentenac 2002). No homologous genes to *OsTPC1* were found in the whole rice genome and expression of its mRNA was ubiquitously observed in various organs and cultured cells (Fig. 2). OsTPC1 may function as a one of the major voltage-gated Ca^{2+} channels in rice.

Functions of OsTPC1 in regulation of growth and development

OsTPC1-overexpressing plants displayed reduced growth rate and dwarf phenotype (Fig. 4C). Dwarfism is frequently observed in stress-tolerant plants. For example, transgenic plants overexpressing a stress-inducible transcription factor *DREB1A* become tolerant to freezing and dehydration, resulting in severe reduction in plant size (Liu et al. 1998). Overproduction of stress-related proteins under unstressed conditions may lead to growth retardation of the plants. Since cytosolic free Ca^{2+} serves as an important second messenger participating in transduction of various environmental stress signals to induce expression of a variety of stress-related proteins (Sanders et al. 2002), overproduction of the plasma membrane Ca^{2+} channels may result in enhancement of stress-induced mobilization of $[Ca^{2+}]_{cyt}$ leading to overproduction of stress-related proteins. Therefore dwarfism observed in *OsTPC1*-overexpressing plants may be attributed to hypersensitivity to environmental stresses.

One line (S2-3) in which the expression level of *OsTPC1* was highest showed most severe phenotype including a death symptom (Fig. 4C). Overproduction of plasma membrane Ca^{2+} channels may induce mobilization of excess amount of Ca^{2+}, to cause drastic toxic symptoms.

Possible involvement of OsTPC1 in the chloroplast development

Elevation of $[Ca^{2+}]_{cyt}$ have also been shown to play important roles in developmental and morphogenetic processes, such as elongation, formation of polarity and differentiation of cells (White and Broadley 2003). For example, localized elevation of $[Ca^{2+}]_{cyt}$ in the apical side of the cell is shown to control polarized growth of a pollen tube (Malho and Trewavas 1996). Voltage-gated Ca^{2+}-permeable channel-induced spatiotemporal changes in $[Ca^{2+}]_{cyt}$ are suggested to be crucial for regulation of cell volume in *Fucus* rhizoid and cell elongation in roots (Taylor et al. 1996, Kiegle et al. 2000, Foreman et al. 2003).